Type Ia SNe along redshift: the $\mathcal{R}$(Si II) ratio and the expansion velocities in intermediate z supernovae

G. Altavilla [1], P. Ruiz–Lapuente [1,2], A. Balastegui [1], J. Méndez [1,3], M. Irwin [4], C. España–Bonet [1], K. Schahmaneche [5], C. Balland [5], R. S. Ellis [4,6], S. Fabbro [7], G. Folatelli [8], A. Goobar [8], W. Hillebrandt [2], R. M. McMahon [4], M. Mouchet [5], A. Mourao [7], S. Nobili [8], R. Pain [5], V. Stanishev [8], N. A.Walton [4]

Received _____; accepted _____

Running title: Type Ia SNe along redshift

[1]Departament of Astronomy, University of Barcelona, Diagonal 647, E–08028 Barcelona, Spain

[2]Max–Planck Institut für Astrophysik, Karl Schwarzschildstrasse 1, D-85741 Garching, Germany

[3]Isaac Newton Group of Telescopes, 38700 Santa Cruz de La Palma, Islas Canarias, Spain

[4]Institute of Astronomy, University of Cambridge, Madingley Road,Cambridge. CB3 0HA, United Kingdom

[5]LPNHE, CNRS–IN2P3 and Universities of Paris & 7, F–75252 Paris Cedex 05, France

[6]California Institute of Technology, Pasadena. CA 91125, USA

[7]CENTRA–Centro M. de Astrofisica and Department of Physics, IST, Lisbon, Portugal

[8]Department of Physics, Stockholm University, SE–10691 Stockholm, Sweden

ABSTRACT

We study intermediate–z SNe Ia using the empirical physical diagrams which enable to learn about those SNe explosions. This information can be very useful to reduce systematic uncertainties of the Hubble diagram of SNe Ia up to high z. The study of the expansion velocities and the measurement of the ratio $\mathcal{R}$(Si II) allow to subtype SNe Ia as done in nearby samples. The evolution of this ratio as seen in the diagram $\mathcal{R}$(Si II)–(t) together with $\mathcal{R}(\mathrm{Si\,II})_{max}$ versus $(\mathrm{B\text{-}V})_0$ indicate consistency of the properties at intermediate z compared with the nearby SNeIa. At intermediate–z, expansion velocities of Ca II and Si II are found similar to those of the nearby sample. This is found in a sample of 6 SNe Ia in the range $0.033 \leq z \leq 0.329$ discovered within the *International Time Programme* (ITP) of SNe Ia for Cosmology and Physics in the spring run of 2002 [9]. Those supernovae were identified using the 4.2m William Herschel Telescope. Two SNe Ia at intermediate z were of the cool FAINT type, one being a SN1986G–like object highly reddened. The $\mathcal{R}$(Si II) ratio as well as subclassification of the SNe Ia beyond templates help to place SNe Ia in their sequence of brightness and to distinguish between reddened and intrinsically red supernovae. This test can be done with very high z SNe Ia and it will help to reduce systematic uncertainties due to extinction by dust. It should allow to map the high–z sample into the nearby one.

Subject headings: supernovae: general – supernovae: individual: 2002li, 2002lj,

[9]The programme run under *Omega and Lambda from Supernovae and the Physics of Supernova Explosions* within the *International Time Programme* at the telescopes of the *European Northern Observatory* (ENO) at La Palma (Canary Islands, Spain)

2002lk, 2002ln, 2002lo, 2002lp, 2002lq, 2002lr, – cosmology: observations

1. Introduction

The measurements using Type Ia Supernovae of the expansion rate of the Universe led to the discovery of its acceleration (Riess et al. 1998; Perlmutter et al. 1999) and has opened a new field in the identification of the driving force of the accelerated expansion, the so called dark energy. A large local supernova sample was first studied in the Calan–Tololo survey (Hamuy et al. 1996) and nowadays in a series of campaigns at low redshift by various collaborations. At high-z, the first supernova samples were gathered by the Supernova Cosmology Project (Perlmutter et al. 1999; Knop et al. 2003; Hook et al. 2005) and the High–Z SN team/ESSENCE (Riess et al. 1998; Tonry et al. 2003; Barris et al. 2004; Krisciunas et al. 2005; Clocchiatti et al. 2005). In the last years, the high–z redshift range has been targeted as well by the Supernova Legacy Survey (Astier et al. 2005). The combination of the discoveries made by all these collaborations will provide hundreds of SNe Ia at z$>$ 0.2. At very high–redshift, the Higher–Z Team using the *Hubble Space Telescope* concentrates in the discovery of supernovae at z$>$ 1 to better constraint dark energy (Riess et al. 2005). This is also the target of the latest runs of the Supernova Cosmology Project which is presently studying SNe Ia in galaxy clusters at very high z.

While the low and high redshift intervals are often targeted, the intermediate redshift ($0.1 \lesssim z \lesssim 0.4$) region is still an almost unexplored zone. We started a programme to have a well covered sample of SNe Ia between z$\sim$ 0.1 and z$\sim$ 0.4. In this paper, we present the spectroscopic results of the observations done in spring 2002, of the ITP project on supernovae for their physics and cosmology (P.I. Ruiz–Lapuente)[10]. We discuss where these supernovae stand in the empirical physical diagrams used to describe the supernova

[10]The programme run in 2002 under *Omega and Lambda from Supernovae and the Physics of Supernova Explosions* within the *International Time Programme* at the telescopes of the *European Northern Observatory* (ENO) at La Palma (Canary Islands, Spain)

density profile and temperature. The results of the photometric follow–up and their cosmological implications will be presented in a forthcoming paper. There are prospects that SDSS–II (Sako et al. 2005a,b) will provide a large sample of SNe Ia at those z while the SNFactory (Aldering et al. 2004) will concentrate in supernovae at z $\sim$ 0.1. At ENO, our own collaboration plans to move to very high–z to carry campaigns that will explore the physics of SNe Ia in detail at those high–z in a similar way as done for the nearby sample. Physical properties of SNe Ia can be better studied within intensive supernova campaigns by collecting a large database of spectra and photometry for each individual supernova. This task has been the aim of the RTN on Physics of Type Ia supernovae which compares each single SNIa with model spectra to better understand SNe Ia explosions (Hillebrandt et al. 2005). Detailed spectral evolution provides a complete probe of the SNe Ia ejecta: chemical composition, velocity and other physical characteristics of the layers that successively become transparent.

At high–z, the observing time per supernova has to be optimised. Long exposure times are needed to obtain good S/N spectra for the large amount of candidates in the supernova searches. This prevents from having a complete sequence of spectra. However, as we will show here, one can go a step beyond what has been done up to now with high–z SN spectra and do a finer classification. In this intermediate–z campaigns (see Ruiz–Lapuente 2006 for a review), we have seen how information similar to the one gathered in nearby SNe Ia can be gathered at all z.

Spectral studies of intermediate z supernovae have started to incorporate the study of expansion velocities of the material within the ejecta (Altavilla et al. 2005; Balastegui et al. 2005; Mendez et al. 2005; Balland et al. 2006). The intermediate redshift spectra gathered offer here the possibility of investigating where the SNe Ia stand in distribution of chemical elements in the velocity space and the temperature within the ejecta (Branch et

al. 1993a; Hatano et al. 2000; Benetti et al. 2004; Benetti et al. 2005; Branch et al. 2006). This opens a new window inside the supernova ejecta and allows to test the existence of continuity in the temperature and spatial gradient characteristics of SNe Ia. Ultimately, these intermediate redshift Type Ia SNe will help to fill the gap between the local and high–z SN samples, reducing the statistical uncertainties by means of an evenly sampled Hubble diagram. These supernovae are to be used in cosmology in conjunction with those gathered by other surveys.

The outline of the paper is as follows. In section 2 we present the observations and the data reduction procedure, and in section 3 the SN candidates classification. In section 4 we comment the results on individual objects and bring them into comparison with the nearby sample. Matches of the spectra to nearby SNe Ia are examined. In section 5 the physical diagrams for intermediate z SNe Ia are first buildt up in a way similar to what is done in nearby SNeIa. The prospects to use these diagrams to reduce systematic uncertainties are shown. Further discussion is presented in section 6. A brief summary of the run and conclusions are reported in section 7.

2. Observations and data reductions

Spectra of the SN candidates were obtained using the 4.2-m William Herschel Telescope (WHT)[11]. Observations were done using the spectrograph ISIS on June 10^{th} and 11^{th}, 2002 (Table 1). A dichroic allowed to carry simultaneous observations in the blue and red channels, which are optimised for their respective wavelength ranges (∼3000–6000 Å, ∼5000–10000 Å). In the blue, the R158B grating was used in conjunction with the EEV12

[11]The WHT is operated by the Isaac Newton Group of Telescopes (ING), located at the Roque de Los Muchachos Observatory, La Palma, Spain

detector. In the red, we used the R158R grating + GG495 filter[12] and the MARCONI2 detector. In the red channel fringing begins at about 8000 Å and increases to ∼10 per cent at 9000 Å. A longslit of 1.2 arcseconds was used in the first night, under good weather conditions, and a longslit of 1.03 arcseconds was adopted in the second night, under excellent weather conditions (except for SN 2002lk and one spectrum of SN 2002lj, which were observed at the beginning of the night with a 1.2" slit). A journal of the spectral observations is given in Table 1.

Spectra were reduced following standard IRAF [13] procedures. All images were bias subtracted and then flat fielded using dome flats. The one dimensional spectrum extractions were weighted by variance based on the data values and a Poisson/CCD model using the gain and read noise parameters. The background was interpolated by fitting two regions beside the spectra and then subtracted. Reference spectra of Cu-Ne-Ar lamps were used for the wavelength calibration. The results were checked measuring the position of bright [O I] sky lines at 5577 Å and 6300 Å and, when necessary, a rigid shift was applied to the spectrum to be consistent with these values. The spectra were flux calibrated using spectrophotometric standard stars observed at the start and at the end of each night. Correction for atmospheric absorption was applied to the red arm spectra. The blue and the red sections were joined in a single spectrum and multiple spectra of the same object

[12]An order-separation filter designed to filter out second order blue from the first order red in usual applications, in the case of ISIS, where a dichroic splits the beam into red and blue channels, it helps define the 'red' channel short wavelength

[13]http://iraf.noao.edu/

IRAF is distributed by the National Optical Astronomy Observatories (NOAO), which are operated by the Association of Universities for Research in Astronomy (AURA), Inc., under cooperative agreement with the National Science Foundation.

were then combined in order to improve the signal to noise ratio. Spectra with different exposure times were weighted accordingly.

3. Classification

3.1. Object, redshift and phase determination

Spectra can be inspected visually in order to give a rough classification of the SN candidate, where the main feature used to discriminate between Type Ia, Type II SNe or 'other' sources (typically QSOs or AGN) is the presence/absence of the strong Si II absorption at ∼6150 Å (rest-frame) and the typical S II ∼5400 Å (rest–frame) 'W' feature for Type Ia SNe. Type II SNe show the characteristic Balmer series P–Cygni profiles, most noticeably the H_α spectral feature. For a correct classification, one has to be aware of the possible confusion between SNe Ia and SNe Ic. This possibility increases its chances for cool SNIa events when only one spectrum is available. As it will be shown in this paper, such possibility can be reduced if one uses the physical diagrams (expansion velocity and $\mathcal{R}$(Si II)) in intermediate and high–z SNe Ia. For all those reasons and to find the best match in a library of SNe Ia, it is required to follow an automatic procedure that will enable to size the difference of the spectra of the SNe Ia with those of an archive from a large sample of nearby SNe Ia at all phases.

The redshift of the supernova is obtained from the redshift of the galaxy lines. In case of no emission lines, it can be obtained by the algorithm. In our sample, the spectra were inspected looking for typical narrow galaxy lines: Balmer lines, [O II] λ3727, [O III] λ5007, [N II] λ6583, [S II] λ6716, 6731). Images of the host galaxy of the supernovae are shown in Figures 1, 3, 5, 7, 9, and 11 and figures of the supernova spectra with the emission lines of the underlying host galaxy are shown in Figures 2, 4, 6, 8, 10, and 12 (top panels). The

lines used for the redshift determination (when present) are shown. Uncertainties on the redshifts are of the order of 0.001 and they have been estimated measuring the dispersion of the redshift determinations obtained from each identified galaxy line.

The following step was taken to refine the Type Ia SN classification by means of two different classification algorithms developed to this aim. The first classification program transforms the spectra into rest–frame and compares it to a set of Type Ia supernovae spectral templates originally prepared by Nugent, Kim, & Perlmutter (2002), and later adapted by Nobili et al. (2003). These spectral templates range from 19 days before maximum to 70 days after maximum, and the wavelength coverage is from 2500 Å to 25000 Å. Both the spectra and the templates are normalized in the wavelength range selected for the comparison, and then the spectra are again rescaled and shifted in the flux axis until the best match is found, see Figs. 2, 4, 6, 8, 10, and 12 (middle panels) This procedure uses the whole spectrum and the result is not based on a few key features only.

In an interactive mode, the algorithm asks for a smoothing length and a σ level to clean spikes in the observed spectrum. In this second mode, the procedure allows the user to specify the wavelength interval or to reject wavelength intervals of the comparison spectrum. This can be useful to reject a region of the spectrum highly contaminated with atmospheric absorption lines. Finally, the user can select the interval of redshifts and epochs used in the comparison.

Mathematically the algorithm works by finding the minimum χ^2 of the observed spectrum compared with spectra of all the possible values of the epoch, j, and the redshift, z:

$$\chi^2_j(z) = \sum_{i=1}^{n} \frac{[f(\lambda_i) - F_j(\lambda_i, z)]^2}{{\sigma_i}^2} \tag{1}$$

where n is the total number of data points of the observed SN spectrum, $f(\lambda_i)$ is the

SN normalized flux at wavelength λ_i, and $F_j(\lambda_i, z)$ is the template normalized flux at wavelength λ_i, epoch j, and redshift z. The algorithm delivers rest–frame epoch, flux scale and redshift as parameters. If the redshift is known from the narrow galaxy lines, the algorithm takes it as given and the redshift is not used in the minimization.

Once the first classification is obtained based on templates, a second analysis is done using an algorithm that compares the SNe Ia with those of the Padova SN Catalogue and other spectra available in the literature (we also made use of the SUSPECT database[14]). This allows to find a real template which best fits the SN Ia (Figs. 2, 4, 6, 8, and 10, lower panel). The two algorithms *Genspecphase* and *Genspecsubtype* were developed for this programme and can be used in campaigns at all redshifts. Results with the redshift z and phase determination can be seen in Table 2.

We estimated the spectral epoch and its uncertainty by comparing the phases obtained matching the spectra with the synthetic and real templates. We assumed a minimum error of ± 2 days (see also Riess et al. 1997). The comparison of the spectral phase τ_{spec} with the phases τ_{pho} determined from the photometric data (see Table 2) shows that the spectral epochs are correct within a few days, with a scatter of $\sigma = 3.5$ days (Fig. 13). This value is consistent with the adopted spectroscopic phase error bars.

SN 2002lk presented an interesting test for classification. It was an intrinsically red (cool) SNIa and in addition to it, it is highly reddened. A rough approach might have mistaken it for a SNIc at another phase. We included a number of intrinsically red (cool) SNeIa in our database as well as Type Ic supernovae to increase the quality of the classification. Consistency is found with the color light curves and the spectral classification.

Observed and template spectra have been smoothed and tilted with an absorption amount

[14]http://bruford.nhn.ou.edu/∼suspect/index1.html

derived empirically within the classifying procedure. This 'reddening factor' may not be totally due to absorption, and it is applied to correct for light losses due to observations with the slit out of the parallactic angle and/or to take into account different colours between targets and templates, and/or to take into account reddened templates. In some cases the spectral templates have been slightly red- or blueshifted to account for the small differences in the expansion velocities between the template and the observed SN.

The peculiar Type Ia SN 2002lk and Type II supernovae have been compared with real templates only (Figs. 12, 14, 15).

Table 3 summarizes the results of the classification of the host galaxies of all SN candidates.

3.2. Host galaxy morphology

Host galaxy morphology identification is usually done exploiting good imaging and spectra (Sullivan et al. 2003). In our sample, a certain visual identification of the host galaxy morphology is feasible for two objects only: SN 2002lq (Fig. 7), and SN 2002lk (Fig. 11). The latter is a Type Ia SN similar to the underluminous SN 1986G, which exploded in a spiral galaxy (for a discussion on the host galaxies of subluminous SNe, see Howell 2001). This galaxy has been classified as spiral since its ellipticity, larger than 7, is not consistent with an elliptical galaxy and, although it is observed almost edge on, the existence of some structure, as a dust lane, can be detected. An image of the galaxy about one year after explosion reveals also the bulge of the galaxy, hidden in Fig.11 by the SN light.

The rest of the galaxy images do not give hints on the galaxy morphology, being compatible with both elliptical and spiral galaxies (in the latter case the possible spiral structure is unresolved) (Figs. 1, 3, 5, and 9). Since we have no spectra of the host

galaxies alone, the identifications given are made exclusively on the basis of the galaxy lines contaminating the SNe spectra (Kennicutt 1992). Thus, we will only distinguish between spheroidal galaxies (ellipticals and lenticulars) and spiral galaxies (without giving any further subclassification).

SN 2002li and SN 2002lq host galaxies are classified as spiral galaxies, since they have a good number of lines from the Balmer series. The host galaxy morphology of the SN 2002lq host can be also inferred from visual inspection, while SN 2002li host galaxy structure is not as clear as the previous case.

SN 2002lj lacks galaxy lines. Without any clear Balmer emission line, we have classified it as a spheroidal galaxy.

SN 2002lp has Hα, Hγ and Hθ in emission, but very faint. Its host galaxy is possibly spiral. The spectrum of SN 2002lr presents also narrow emission lines.

The Type II SNe, SN 2002ln and SN 2002lo, show narrow emission lines of the Balmer series. Their host galaxies have been classified as spirals (Table 3).

4. Spectroscopic classification

4.1. Type Ia Supernovae

SN 2002li

This is the farthest supernova discovered in this search ($z = 0.329$). Fig. 2 (bottom panel) shows the comparison with SN 2000E (Valentini et al. 2003), a SN spectroscopically almost identical to SN 1990N, i.e. a typical Type Ia SN. Both the comparison with SN 2000E and Nobili's spectral templates (Fig. 2, middle panel) suggest that the SN 2002li phase corresponds to a few days before maximum.

The blue-shifted H and K lines at 3950 Å indicate that the expansion velocity of Ca II in SN 2002li is ∼17200 km s^{-1}, lower than for SN 2000E (∼21000 km s^{-1}). The signal to noise ratio does not allow a reliable determination of the expansion velocity of Si II at ∼6150 Å . Photometric data suggest that SN 2002li is a slow decliner object ($\Delta m_{15}(B) \sim 0.79 \pm 0.22$), but being spectroscopically normal. In the local sample, slow decliners are often normal spectroscopically (Hamuy et al. 2002).

SN 2002lj

The redshift of SN 2002lj has been derived from SNe features due to the absence of measurable galaxy emission lines. Both the match with a real SN (SN 1994D, Patat et al. 1996) (Fig. 4, bottom panel) and a template spectrum (Fig. 4, middle panel) suggest that the observed epoch for SN 2002lj is about a week past maximum. Since SNeIa still show S II features between 5500 Å and 5700 Å 7 days after maximum, the absence of these features in the SN 2002lj spectrum suggests a phase between 7 and 10 days past maximum. The redshift was found by comparison with the template SN features, thus most of them have the same expansion velocity, except Si II at 6355 Å, whose expansion velocity for SN 2002lj is lower (∼8900 km s^{-1}) than the one measured for SN 1994D (∼9800 km s^{-1}).

SN 2002lp

The finding chart for this SN (Fig. 5) shows the large offset from the host galaxy. The comparison of the spectra of SN 2002lp with that of 1989B at maximum (Barbon et al. 1990; Wells et al. 1994) shows that they are quite similar (Fig. 6, bottom panel). The match with a template at day 3 after maximum (Fig. 6, middle panel), confirms that the spectrum of SN 2002lp was taken close to maximum. The expansion velocity measured from the Si II unresolved doublet 6355 Å (∼10400 km s^{-1}) is almost coincident with the

one measured for SN 1989B (∼10000 km s^{-1}). The absorption dip at ∼5800 Å, identified as Si II 5972 Å, is stronger than in SN 1989B. This is quantified by the $\mathcal{R}$(Si II) parameter, or ratio of the two Si II absorptions dips, i.e. the one at ∼5800 Å and the one at ∼ 6150 Å (Nugent et al. 1995). In SN 2002lp, $\mathcal{R}$(Si II) is 0.50 ± 0.05 and in SN 1989B is 0.29 ± 0.05 for the same period.

The match with a template at day 3 after maximum, confirms that the spectrum of SN 2002lp was taken near maximum. The expansion velocities measured from the Si II unresolved doublet (6355 Å) and Ca II lines (3950 Å) (∼10400 km s^{-1}, ∼13800 km s^{-1} respectively) are almost coincident with the ones measured for SN 1981B (∼10400 km s^{-1}, ∼14000 km s^{-1}). While the velocities for SN 2002lp are in the range of those found in SN1981B, the absorption dip at ∼5800 Å, identified as Si II 5972 Å, is stronger than in SN 1981B. In SN 1981B, $\mathcal{R}$(Si II) is 0.16 ± 0.05 near maximum, a value which is typical for normal SNe Ia. The spectral comparison with the complete SNe Ia library finds that SN 1989B is the best match for this supernova (Fig. 6, bottom panel).

SN 2002lq

The Si II (6355 Å) feature if existent, is very faint but the comparison with SN 1990N, a typical SN Ia with good spectral coverage (Leibundgut et al. 1991), suggests that SN 2002lq is a Type Ia SN observed about one week before maximum (Fig. 8, bottom panel). Matching synthetic templates gives a phase of 7 days before maximum for this supernova (Fig. 8, middle panel). The only well visible feature in this low S/N spectrum is Ca II line at 3950 Å, and its expansion velocity (∼18900 km s^{-1}), measured with large uncertainty, seems somewhat lower than that of SN 1990N (∼21000 km s^{-1}).

SN 2002lr

This Type Ia supernova was observed about 10 days after maximum, as derived from fitting the templates and fitting to real SNe Ia (Fig. 10, middle and bottom panels). SN 2002lr spectrum is similar to one of SN 1994D (Patat et al. 1996) 10 days past maximum. The expansion velocity derived from Si II (6355 Å) ($\sim$8600 km s^{-1}) is similar to the one derived for SN 1994D ($\sim$9500 km s^{-1}). The expansion velocity measured from the Ca II line at 3950 Å is $\sim$12800 km s^{-1} but it is not possible to compare this value with the corresponding one in SN 1994D because the limited spectral range of the template does not allow the measurement of the Ca II line.

SN 2002lk

For SN 2002lk two different spectra are available since it was observed in two consecutive nights (Fig. 12). The strong similarities between the spectra of SN 2002lk and SN 1986G (Phillips et al. 1987); Padova SN Catalogue), suggest that SN 2002lk is a SN 1986G–like event observed a few days before maximum. Due to the spectrum peculiarities, a comparison with Nobili's spectral templates is not appropriate. In Fig. 12, the spectra of SN 1986G have been shifted in wavelength in order to match better that of SN 2002lk. This small shift takes into account the different expansion velocities of the two objects. For SN 2002lk the velocity determined from the Si II line at 6355 Å is $\sim$14500 km s^{-1}, while for SN 1986G is $\sim$10800 km s^{-1}. The significant difference between the two values may be attributed to different explosion energy. SN 2002lk is characterized by higher expansion velocity, slower decline rate in the B light curve ($\Delta m_{15}(B) \sim 1.23 \pm 0.02$), and similar $\mathcal{R}$(Si II) with respect to SN 1986G. Thus, SN 2002lk, in its turn, can be considered a less extreme object with respect to SN 1986G, suggesting a continuous transition from object to object. We notice that similar high expansion velocity was found for SN 1998de, a 1991bg-like SN (Modjaz et al. 2001), whose expansion velocity (6 days before maximum) derived from the Si II (6355

Å) minimum was 13300 km s^{-1} (Garnavich, Jha, & Kirshner 1998).

As far as reddening is concerned, the detection of the Na ID ($\lambda\lambda$5890, 5896 Å) allows us to estimate the host galaxy component of the color excess $E(B-V)$. The host galaxy is a spiral galaxy and the supernova is highly reddened by the galaxy dust lane. By means of an empirical relation between the equivalent width (EW) of the Na ID lines and $E(B-V)$ (Barbon et al. 1990; Richmond et al. 1994; Turatto, Benetti, & Cappellaro 2003) we estimated $E(B-V) \simeq 0.15 - 0.5$ ($A_V \simeq 0.46 - 1.55$), where the two values correspond to two different slopes of the relation found by Turatto, Benetti, & Cappellaro (2003). The colour excess $E(B-V) = 0.56 \pm 0.04$ derived from the photometric data is consistent with the value obtained from the spectroscopic analysis. The Galactic component of the absorption is quite negligible: $A_V = 0.025$ (Schlegel, Finkbeiner, & Davis 1998). The spectrum of SN2002lk has a very flat bottom Ca II and Si II absorption troughs. The shape of those absorptions suggest that this is a highly asymmetric supernova, like SN 2004dt.

4.2. Type II Supernovae

SN 2002ln and SN 2002lo

Both Type II SNe are matched with SN 1999em as template, a normal Type II Plateau (Elmhamdi et al. 2003). The phase is not so well defined for SN 2002ln since the blue part of the spectrum has a low S/N. A comparison of SN 2002ln with SN 1999em at 9, 14 (Hamuy et al. 2001), and 24 (Leonard et al. 2002) days since B maximum, shown in Fig.14, suggests a phase of about 2 weeks. The H_α minimum is not measurable, the peak of the P-Cygni profile, in principle expected to be at null velocity, is slower in SN 2002ln ($\sim$220km s^{-1} for SN 2002ln, $\sim$2500km s^{-1} for SN 1999em).

A comparison with SN 1999em $\sim$35 days since B maximum (Leonard et al. 2002)

shows that SN 2002lo is about one month old (Fig. 15). The expansion velocity measured from the H_α minimum in SN 2002lo ($\sim$8980km s^{-1}) is slightly higher than the one measured for SN 1999em ($\sim$6100km s^{-1}) (Fig. 16), while the peak of the P-Cygni profile is faster for SN 2002lo ($\sim$1500km s^{-1}) with respect to SN 1999em ($\sim$950km s^{-1}). Uncertainties for our measurements are of the order of 500 km s^{-1}. However Type II Plateau SNe, and Type II SNe in general, are a very heterogeneous class, showing a wide range in the photometric and spectroscopic properties (Patat et al. 1994; Filippenko 1997).

5. $\mathcal{R}$(Si II) parameter & Expansion velocities

Several diagrams can help us to learn about these intermediate–z SNe Ia as explosions and allow a comparison with the nearby sample. Expansion velocities for Ca II (3950 Å) and Si II (6355 Å) lines have been measured from the blueshift of the lines, as in the local sample. The ratio of the two Si II lines, i.e. Si II (6355 Å) and Si II (5890 Å) defines the $\mathcal{R}$(Si II) parameter as introduced by Nugent et al. (1995). We measure in this exploration the $\mathcal{R}$(Si II) parameter following these authors: drawing segments between adjacent continuum points of the absorption lines and measuring the difference in flux between the higher excitation transition of the two (those transitions are the 4P–5S and the 4S–4P). If the photosphere has a higher effective temperature *Teff*, one would expect that the 5800 Å trough would increase towards higher *Teff*. The behavior in SNe Ia is, however, twofold at very early phases (Fig. 17). In one group, $\mathcal{R}$(Si II) is seen to increase significantly towards the premaximum, hotter phase. This is found in SNe Ia like SN2002bo and SN2004dt which present significant 5800 Å troughs compared to the one at 6150 Å in this premaximum phase, while in another group it is the opposite: $\mathcal{R}$(Si II) decreases towards the premaximum hotter phase in SNe Ia like SN 1990N or stays constant like in SN2003du. Such diversity of behaviors could be linked to the presence of Fe and Co in the outer layers. According

to Nugent et al (1995), the Si II lines interact with line blanketing from Fe III and Co III at premaximum when the temperature is high and Fe and Co are substantially present in the outer layers. This effect washes out the 5800 Å trough. The decrease of $\mathcal{R}(\mathrm{Si\,II})$ at premaximum in SN 1990N could be due to Fe and Co in the outer layers, as this supernova showed these elements in the premaximum spectra. The supernovae which behave like SN 2004dt and SN2002bo do not have substantial Fe in the outer layers. An independent analysis points in that direction for SN2004dt. In SN 2002bo, intermediate–mass elements were most abundant in the outer layers (Stehle et al. 2004). The high $\mathcal{R}(\mathrm{Si\,II})$ is consistent with the expectation of minor line blanketing by FeIII and CoIII.

While we have discussed this ratio at premaximum, which could be an indicator of the physics of the outer layers, we have that at maximum the time evolution in $\mathcal{R}(\mathrm{Si\,II})$ is quite flat, and one can define $\mathcal{R}(\mathrm{Si\,II})_{max}$. The blanketing by Fe III and Co III at this epoch is likely negligible as such ionization stages are not found with the lower temperatures at maximum. In that epoch $\mathcal{R}(\mathrm{Si\,II})_{max}$ correlates well with absolute magnitude: the more luminous the SNe Ia the lower the $\mathcal{R}(\mathrm{Si\,II})_{max}$ and the fainter the SNe Ia the higher the $\mathcal{R}(\mathrm{Si\,II})_{max}$. We have investigated in Figure 18 the $\mathcal{R}(\mathrm{Si\,II})_{max}$ ratio versus intrinsic color of the supernova. We find that the bluer SNe Ia have smaller $\mathcal{R}(\mathrm{Si\,II})_{max}$. We have placed our intermediate z SNe Ia in that Figure and obtained that those intermediate–z SNe Ia are within the trend defined by nearby SNe Ia. For consistency of our comparison between the intermediate z sample and the nearby sample, $\mathcal{R}(\mathrm{Si\,II})$ ratio has been measured in a similar way. In both cases, we follow Nugent et al. (1995) in defining the continuum and the minimum of the absorption throughs. The E(B-V) in the nearby sample is measured using the Lira–Phillips relation (Lira 1995; Phillips et al. 1999) for the tail of the B-V color, which allows to determine the excess E(B–V) by comparison of the tail from 30 to 60 days after maximum with the tail of unreddened SNe Ia (the tail in that epoch shows very low dispersion). In the intermediate z SNe Ia, the same has been done when observations after

maximum were available and, in the absence of those, we use the color curve for the stretch of the SNeIa (Nobili et al. 2003).

We have been able to measure $\mathcal{R}(\mathrm{Si\,II})_{max}$ for all the SNe Ia found at maximum. In our sample, spectra of two of the SNe Ia were taken one week or more after maximum. Then the Si II 5800 Å trough is replaced by iron lines and $\mathcal{R}(\mathrm{Si\,II})_{max}$ can not be measured. In the premaximum SN 2002lq the S/N level does not allow to measure this ratio. It has been possible to obtain a good measurement of this ratio for SN 2002lk and SN 200lp and measured with larger error bars for SN2002li (see Table 4). Fig. 17 shows the ratio $\mathcal{R}(\mathrm{Si\,II})$ of the depth of the Si II 5972 and Si II 6355 Å absorption troughs (see Nugent et al. 1995; Benetti et al. 2005). SN2002lp and SN2002lk show remarkable high $\mathcal{R}(\mathrm{Si\,II})$ values a few days before maximum in consistency with what is found for red, faint SNIa. SN 2002li has values for $\mathcal{R}(\mathrm{Si\,II})_{max}$ consistent with what is found from SNe Ia of the same brightness in the nearby sample.

6. Discussion

The spring run of the ITP 2002 on SNe Ia for Cosmology and Physics gave 6 Type Ia SNe, 2 Type II SNe, 7 quasars and 2 Seyfert galaxies. The redshift range of all the sample is $0.033 \leq z \leq 2.89$ while the SN redshift range is $0.033 \leq z \leq 0.329$. As expected in a magnitude–limited survey, the peak in the redshift distribution of Type II SNe is closer than the peak in redshift of Type Ia SNe. On the other hand, QSO are observed up to very high–redshift (Fig. 19).

Our sample allowed a careful inspection of SNeIa. We have made a comparison of the kinematic and temperature observables in these intermediate–z SNe Ia with those of the nearby sample. Some SNe Ia were intrinsically red and, as in the nearby sample, showed a

large ($\sim$ 0.5 near maximum) $\mathcal{R}(\mathrm{Si\,II})_{max}$ ratio. Other SNe Ia were bluer with $(B-V)_0 <$ 0 near maximum light. Those showed a small $\mathcal{R}(\mathrm{Si\,II})_{max}$ ratio ($\sim$ 0–0.2 near maximum), as in the nearby sample. Amongst the intrinsically red SNe Ia, also called cool SNeIa, we find SN 2002lk and SN2002lp. Those cool SNe Ia are similar to SN 1986G but with less extreme characteristcs (higher expansion velocity, slower decline rate of the B light curve). SN 2002lp is a cool SNIa similiar to SN 1989B. It is a SNIa in between SN1989B and SN1986G. It has a deeper Si II $\sim$5800 Å line and larger $\mathcal{R}(\mathrm{Si\,II})_{max}$ than SN1989B. Both SN 2002lk and SN 2002lp show a similar $\mathcal{R}(\mathrm{Si\,II})$ value ($\sim$0.5). SN 2002lk and SN 2002lp have some other common characteristics: they have the largest $\Delta m_{15}(B)$, they are the closest and the faintest Type Ia SNe. Such trend is in accordance with what could happen under cosmological selection effects.

The interesting aspect shown here is that the intrinsic faintness of the two SNe Ia is not only revealed by a low stretch factor, i.e. high $\Delta m_{15}(B)$, but also from the large $\mathcal{R}(\mathrm{Si\,II})$ values (Nugent et al. 1995; Benetti et al. 2005) which correlate with intrinsic color (see Fig. 18), This fact opens new avenues for a better control over reddening in SNe Ia samples gathered in cosmological surveys.

The expansion velocities measured for all the SNe Ia in this intermediate z sample are consistent with the values measured for nearby SNe (Fig. 20).

From Table 3 we observe that most Type Ia SNe are in spiral galaxies. The 2 Type II observed exploded in spiral galaxies as well. The fraction of Type Ia exploded in spirals amounts to 83 per cent if we take into account the uncertain classification of the host galaxy of SN 2002lp and SN 2002lr. Even if limited by the small statistics and by rough discrimination between spheroidal and spiral galaxies, our result is consistent with the ones derived in a similar redshift range by Valenti et al. (2005) and Balland et al. (2006) (94 and 83 per cent of Type Ia host galaxies are respectively classified as spirals). These values

can be compared to the results derived by Sullivan et al. (2003 and references therein) at low-redshift ($z < 0.01$, 88 per cent) and high-redshift ($0.19 \leq z \leq 0.83$, 71 per cent).

The comparison between the spectral phase determined from the spectral analysis and from the photometric analysis shows a good agreement between the two estimates ($\sigma = 3.5$ days). The agreement gets significantly worse if the time dilation correction (1+z) is not taken into account in the light curve fitting ($\sigma = 5.6$ days).

The time dilation effect is non–neglible at this z range and measurable in those spectra as in high–z SNe Ia.

7. Conclusions

In this paper we present SNe Ia in the desert area of intermediate z, in the redshift range $0.033 \leq$ z ≤ 0.329. The comparison of intermediate z SN spectra with high signal-to-noise ratio spectra of nearby SNe has not revealed significant differences in the spectral features and kinematics. In particular, for all the Type Ia SNe of our sample, included a peculiar one, it has always been possible to find a nearby Type Ia SN counterpart, and the expansion velocities derived from the Si II and Ca II lines are within the range observed for nearby Type Ia SNe. The spectral concordance seems to correspond as well in color and decline of the light curve. The comparison between the epochs determined for each spectrum from the spectral analysis and the photometric epochs derived from fits of the light curves show values in agreement within a few days.

The main conclusion of this research is that the $\mathcal{R}$(Si II) parameter is useful to investigate the physics of SNe Ia explosions at high redshift and serve as meaningful comparison with the nearby SNe Ia sample. It can help to distinguish in the sequence of bright—faint SNe Ia (sequence correlated with slow–fast and with bluer–redder at maximum). It provides a

control over reddening that can be very useful to reduce systematic uncertainties. While in the side of large $\mathcal{R}(\mathrm{Si\,II})_{max}$ one finds faint and intrinsically redder SNe Ia, in the side of low $\mathcal{R}(\mathrm{Si\,II})_{max}$ one finds the intrinsically bluer SNe Ia. We have found that intermediate and nearby SNe Ia follow a similar $\mathcal{R}(\mathrm{Si\,II})_{max}$–(B—V)$_0$ and the intermediate z SNe Ia occupy the same space in the evolution of $\mathcal{R}(\mathrm{Si\,II})$ along time than nearby ones. Similar results are found for the expansion velocity, though a larger sample of SNe Ia at all epochs needs to be investigated.

While the behavior of $\mathcal{R}(\mathrm{Si\,II})$ along time can be linked to luminosity and color properties, there is no trend correlating $\mathcal{R}(\mathrm{Si\,II})_{max}$ with expansion velocities of Si II or Ca II. In the side of large $\mathcal{R}(\mathrm{Si\,II})_{max}$ one can have SNe Ia with a large Si II velocity or with a lower one. Therefore, velocity of the intermediate mass elements is not a tracer of the luminosity according to the present sample. We also have some doubts on the correlation of asymmetries in the ejecta with overall luminosity of the SNIa. SN2002lk is a faint and red SNIa which shows high asymmetries in the Si and Ca lines, while SN 2004dt, a normally luminous SNIa, has those asymmetries as well.

Moreover, the $\mathcal{R}(\mathrm{Si\,II})$ at epochs well before maximum is an observable quantity of great value and accesible to high–z SNeIa searches. While $\mathcal{R}(\mathrm{Si\,II})_{max}$ correlates well with intrinsic color, $\mathcal{R}(\mathrm{Si\,II})_{premax}$ can identify the composition of the outer layers of the SNeIa observed in cosmological searches. Thus, with the same spectra obtained in the discovery runs one can investigate the nature of those explosions.

Acknowledgments

This research was carried through the International Time Programme *Omega and Lambda from Supernovae and the Physics of Supernova Explosions* at the ENO Observatory

and it is based on observations made with the 4.2-m William Herschel Telescope, operated on the island of La Palma by the Isaac Newton Group in the Spanish Observatorio del Roque de los Muchachos of the Instituto de Astrofisica de Canarias. Thanks are given to the scientific staff of the Observatory in Padova, and specially to Stefano Benetti. This work is supported in part by the European Community's Human Potential Programme under contract HPRN–CT–2002–00303, *The Physics of Type Ia Supernovae*.

REFERENCES

Altavilla G. et al. 2005, in Turatto M, Benetti S., Zampieri L., Shea W., eds, ASP Conf. Ser. Vol. 342, 1604-2004: Supernovae as Cosmological Lighthouses. Astron. Soc. Pac., San Francisco, p. 486

Aldering, G. et al. 2004, Proceedings of SPIE, 4836, 61

Astier, P. et al. (The SNLS Collaboration) 2005, A & A (in press)

Balastegui A. et al. 2005, in Turatto M, Benetti S., Zampieri L., Shea W., eds, ASP Conf. Ser. Vol. 342, 1604-2004: Supernovae as Cosmological Lighthouses. Astron. Soc. Pac., San Francisco, p. 490

Balland C. et al., 2006, A&A, 445, 387

Barbon R., Benetti S., Cappellaro E., Rosino L., Turatto M. 1990, A&A, 237, 79

Barris B.J. et al., 2004, ApJ, 602, 571

Benetti S. et al., 2004, MNRAS, 348, 261

Benetti S. et al., 2005, ApJ, 623, 1011

Blanton E.L., Schmidt B.P., Kirshner R.P., Ford C.H., Chromey F.R., Herbst W. 1995, AJ, 110, 2868

Branch D., van den Bergh S. 1993, AJ, 105, 2231

Branch D., Fisher A., Nugent P. 1993, AJ, 106, 2383

Branch D., Dang, L. C., Hall, N., Ketchum, W., Melakayil, M., Parrent, J., Troxel, M. A., Casebeer, D., Jeffery, D. J. & Baron E., 2006, astro-ph/0601048

Clocchiatti A. et al. 2005, astro-ph/0510155, accepted for publication in ApJ

Deustua S. et al. 2000, AAS, 196, 3212

Dilday, B. et al. 2005, AAS, 20718005D

Elmhamdi A. et al. 2003 MNRAS, 338, 939

Filippenko A.V. 1989, PASP, 101, 588

Filippenko A.V., 1997, ARA&A, 35, 309

Garnavich P., Jha S., Kirshner R. 1998, IAU Circ. 6980

Hamuy M., Phillips M.M., Suntzeff N.B., Nicholas B., Schommer R.A., Maza J., Aviles R. 1996, AJ, 112, 2398

Hamuy M. et al. 2001, ApJ, 558, 615

Hamuy M. et al. 2002, AJ, 124, 417

Hatano K., Branch D., Lentz E.J., Baron E., Filippenko A.V., Garnavich P.M. 2000, ApJ, 543, 49

Hillebrandt, W., et al. 2005, http://www.mpa-garching.mpg.de∼rtn

Hook I.M. et al. 2005, AJ, 130, 2788

Howell D.A. 2001, ApJ, 554, 193

Jha S., Branch D., Chornock R., Foley R.J., Li W., Swift B.J., Casebeer D., Filippenko A.V. 2006, astro-ph/0602250, submitted to AJ

Kennicutt R.C. 1992, ApJSS, 79, 255

Knop R.A. et al. 2003, ApJ, 598, 102

Krisciunas K. et al. 2005, AJ, 130, 2453

Leibundgut B., Kirshner R.P., Filippenko A.V., Shields, J.C., Foltz C.B., Phillips M.M., Sonneborn G. 1991, ApJ, 371, 23

Li W. et al. 2003, PASP, 115, 453

Lira, P. 1995, Master Thesis, Univ. Chile

Lentz E.J., Baron E., Branch D., Hauschildt P.H., Nugent P.E. 2000, ApJ, 530, 966

Leonard D.C. et al., 2002, PASP, 114, 35

Leonard D.C., Li, W., Filippenko A.V., Foley R.J., Chornock R. 2005, ApJ, 632, 450

Matheson T. et al. 2005, AJ, 129, 2352

Mazzali, P. A., Lucy, L.B, Danziger, I.J., Gouiffes, C., Cappellaro, E. & Turatto, M., 1993, A & A, 269, 423

Méndez J. et al. 2005, in Turatto M, Benetti S., Zampieri L., Shea W., eds, ASP Conf. Ser. Vol. 342, 1604-2004: Supernovae as Cosmological Lighthouses. Astron. Soc. Pac., San Francisco, p. 488

Modjaz M., Li W., Filippenko A.V., King J.Y., Leonard D.C., Matheson T., Treffers, R.R., Riess A.G. 2001, PASP, 113, 308

Nobili S., Goobar A., Knop R., Nugent, P. 2003, A&A, 404, 901

Nugent, P., Kim. A. & Perlmutter,S. 2002, PASP, 114, 803

Nugent P., Phillips M., Baron E., Branch. D., Hauschildt P. 1995, ApJ, 455, 147

Pastorello A. et al. 2005, MNRAS, 360, 950

Patat F., Barbon R., Cappellaro E., Turatto M. 1994, A&A, 282, 731

Patat F., Benetti S., Cappellaro E., Danziger, I.J., della Valle M., Mazzali P.A., Turatto M. 1996, MNRAS, 278, 111

Perlmutter S. et al. 1998, Nature, 391, 51

Perlmutter S. et al. 1999, ApJ, 517, 565

Phillips M.M. et al. 1987, PASP, 99, 592

Phillips M.M., Heathcote S.R., Hamuy M., Navarrete M. 1989, AJ, 95, 1087

Phillips M.M., Lira, P., Suntzeff, N.R., et al. 1999, ApJ, 118, 1766

Pritchet C.J., For The SNLS Collaboration 2005, in Wolff S.C., Laurer T.R., eds, ASP Conf. Ser. Vol. 339, Observing Dark Energy. Astron. Soc. Pac., San Francisco, p. 60

Riess A.G. et al. 1997, ApJ, 114, 722

Riess A.G. et al. 1998, AJ, 116, 1009

Riess A.G., Filippenko A.V., Li W., Schmidt B.P. 1999, AJ, 118, 2668

Riess A.G. et al. 2004, ApJ, 607, 665

Richmond M.W., Treffers R.R., Filippenko A.V., Paik Y., Leibundgut B., Schulman E., Cox C.V. 1994, AJ, 107, 1022

Ruiz–Lapuente P. 2006, in Bernard's Cosmic Stories. Conference held in Valencia, June 2006.

Sako, M. et al. 2005a (astro–ph/0504455)

Sako, M. et al. 2005b, AAS, 207, 15002

Schlegel, D.J., Finkbeiner, D.P., Davis, M. 1998, ApJ, 500, 525

Stehle M., Mazzali, P. A., Benetti, S. & Hillebrandt, W. 2004, MNRAS, 360, 1231

Sullivan M. et al. 2003, MNRAS, 340, 1057

Tonry J.L. et al. 2003, ApJ, 594, 1

Turatto M., Benetti S., Cappellaro E. 2003, in Leibundgut B, Hillebrandt W., eds, Proc. of the ESO/MPA/MPE Workshop: From Twilight to Highlight - The Physics of Supernovae. Springer-Verlag, Berlin, p. 200

Valenti S. et al. 2005, in Turatto M, Benetti S., Zampieri L., Shea W., eds, ASP Conf. Ser. Vol. 342, 1604-2004: Supernovae as Cosmological Lighthouses. Astron. Soc. Pac., San Francisco, p. 505

Valentini G. et al. 2003, ApJ, 595, 779

Wang L., Baade D., Hoeflich P., Wheeler J.C., Kawabata K., Khokhlov A., Nomoto K., Patat F. 2004, astro-ph/0409593, submitted to ApJ

Wells L.A. et al. 1994, AJ, 108, 2233

A. Spectral templates

The spectral analysis has been performed using both synthetic and real spectra. In particular we used 90 synthetic SN Ia spectra by Nobili et al. (2003), based on Nugent's spectral templates (Nugent, Kim, & Perlmutter 2002, `http://supernova.lbl.gov/~nugent/nugent_templates.html`). Phases range from -19 to +70 days since B maximum, with 1 day step. Wavelength coverage is from 2500 Å to 25000 Å, but in our analysis the useful range is limited up to ∼10000 Å. Fig. 21 shows the spectral sequence.

We also made use of real spectral templates, mainly collected from the Padova-Asiago SN Catalogue (Pd-As Cat.) (`http://web.pd.astro.it/supern/snean.txt`, Barbon et al. 1990) and SUSPECT database (`http://bruford.nhn.ou.edu/~suspect/`), spanning a wide range in the decline rates ($\Delta m_{15}(B)$) of the corresponding B band light curves. In particular we used the spectra listed in Table 5. Table 5 shows the spectra available of the comparison SNe Ia that best match our intermediate z ones, while Fig. 22 shows their phase distribution.

Table 1: Journal of spectroscopic observations.

SN	Date (UT)	JD -2400000	Telescope Instrument	Exposure. time (s) Blue Arm	Red arm	Slit arcsec.
2002li	2002 Jun. 10	52436.6	WHT+ISIS	900	900	1.20
	2002 Jun. 10	52436.7	WHT+ISIS	900	900	1.20
	2002 Jun. 10	52436.7	WHT+ISIS	900	900	1.20
2002lj	2002 Jun. 11	52437.4	WHT+ISIS	900	900	1.20
	2002 Jun. 11	52437.4	WHT+ISIS	900	900	1.03
2002lp	2002 Jun. 10	52436.5	WHT+ISIS	900	900	1.20
	2002 Jun. 10	52436.5	WHT+ISIS	900	900	1.20
2002lq	2002 Jun. 10	52436.4	WHT+ISIS	900	900	1.20
	2002 Jun. 10	52436.5	WHT+ISIS	900	900	1.20
2002lr	2002 Jun. 10	52436.7	WHT+ISIS	900	900	1.20
	2002 Jun. 10	52436.7	WHT+ISIS	900	900	1.20
2002lk	2002 Jun. 10	52436.4	WHT+ISIS	300	300	1.20
	2002 Jun. 10	52436.4	WHT+ISIS	600	600	1.20
	2002 Jun. 11	52437.4	WHT+ISIS	600	600	1.20
2002ln	2002 Jun. 10	52436.6	WHT+ISIS	900	900	1.20
	2002 Jun. 10	52436.6	WHT+ISIS	900	900	1.20
2002lo	2002 Jun. 11	52437.6	WHT+ISIS	900	900	1.03
	2002 Jun. 11	52437.6	WHT+ISIS	900	900	1.03

Table 2: Summary of observations.

Object name	Date (UT)	R.A.(2000.0) *hh mm ss*	δ(2000.0) ° ′ ″	Redshift	Object Type	Notes $\tau^{\star}_{spec}$	$\tau^{\diamond}_{pho}$
SN 2002li	2002 Jun. 10	15:59:03.08	+54:18:16.0	0.329	SN Ia	-3±2	-3.31±1.0
SN 2002lj	2002 Jun. 11	16:19:19.65	+53:09:54.2	0.180	SN Ia	+7±2	11.95±0.9
SN 2002lp	2002 Jun. 10	16:40:11.45	+42:28:30.2	0.144	SN Ia	+1±3	-2.45±0.1
SN 2002lq	2002 Jun. 10	16:40:28.83	+41:14:09.1	0.269	SN Ia	-7±2	-10.56±1.3
SN 2002lr	2002 Jun. 10	22:33:12.59	+01:05:56.7	0.255	SN Ia	+10±2	13.47±3.5
SN 2002lk	2002 Jun. 11	16:06:55.92	+55:28:18.2	0.033	SN Ia .	-2±2	-2.90±0.1
SN 2002ln	2002 Jun. 10	16:39:24.93	+41:47:29.0	0.138	SN II	∼14	
SN 2002lo	2002 Jun. 11	16:39:56.42	+42:19:20.5	0.136	SN II	∼35	

* spectral epoch from the spectroscopic analysis

$^{\diamond}$ spectral epoch (rest-frame) from the photometric analysis

Table 3: Host galaxy morphology.

SN Ia	z	Galaxy Type	Offset		Identified lines	*Imaging
2002li	0.329	spiral	0".1 W	0".2 S	H_α, H_β, H_δ, [S II], [N II], [O III], [O II]	y
2002lj	0.180	spheroidal	0".2 W		-	n
2002lp	0.144	spiral?	0".2 E	2".0 N	H_α, H_γ, H_θ, [O II]	n
2002lq	0.269	spiral	4".5 E	0".7 S	H_α, H_β, H_γ, H_δ, H_ζ, H_η, H_θ, [S II], [O III]	y
2002lr	0.255	spiral?	3".0 S		H_β, [S II], [N II], [Ne V]	n
2002lk	0.033	spiral (Sb)	0".7 W	0".2 N	H_α, [S II], [N II], Na D	y
2002ln	0.138	spiral	1".1 W	8".3 S	H_α, H_β, H_ζ, H_θ, [S II]	n
2002lo	0.136	spiral	0".6 E	1".3 S	H_α, H_β, H_θ, [N II], [O III], [O II]	y

⋆ Host galaxy morphology can be inferred (y) or not (n) from visual inspection

Table 4: Expansion velocities for Ca II (3950 Å) and Si II (6355 Å) lines and $\mathcal{R}$(Si II) ratio.

Object name	phase* since B max.	Exp. velocity Ca II (km s^{-1})	Exp. velocity Si II (km s^{-1})	$\mathcal{R}$(Si II)
SN 2002li	-3.31±1.0	17200±500		$0.2^{+0.05}_{-0.10}$
SN 2002lj	11.95±0.9	12300±300	8900±300	
SN 2002lp	-2.45±0.1	13800±900	10400±400	0.50±0.05
SN 2002lq	-10.56±1.3	18900±1400		
SN 2002lr	13.47±3.5	12800±300	8600±400	
SN 2002lk	-2.90±0.1		14500±500	0.50±0.05
SN 2002lk	-1.94±0.1		13850±500	0.46±0.05

* from the light curve fitting

Table 5: SN Ia templates

SN	Type	N. spectra	Time coverage*	$\Delta m_{15}(B)$	Reference(s)	
1986G	Ia pec.	39	-4..+324	1.69(0.05)	Phillips et al. (1987)	Pd-As Cat. - SUSPECT
1989B	Ia	8	0..+52	1.28(0.05)	Barbon et al. (1990)	Pd-As Cat. - SUSPECT
1990N	Ia	6	+2..+333	1.05(0.05)	Leibundgut et al. (1991) Mazzali et al. (1993)	Pd-As Cat. - SUSPECT
1994D	Ia	31	-11..+106	1.31(0.05)	Patat et al. (1996)	Pd-As Cat. - SUSPECT
1999em	II P	40	-1..+515	-	Hamuy et al. (2001) Leonard et al. (2002)	Pd-As Cat. - SUSPECT
2000E	Ia	7	-6..+124	0.94(0.05)	Valentini et al. (2003)	Pd-As Cat. - SUSPECT

* since B maximum

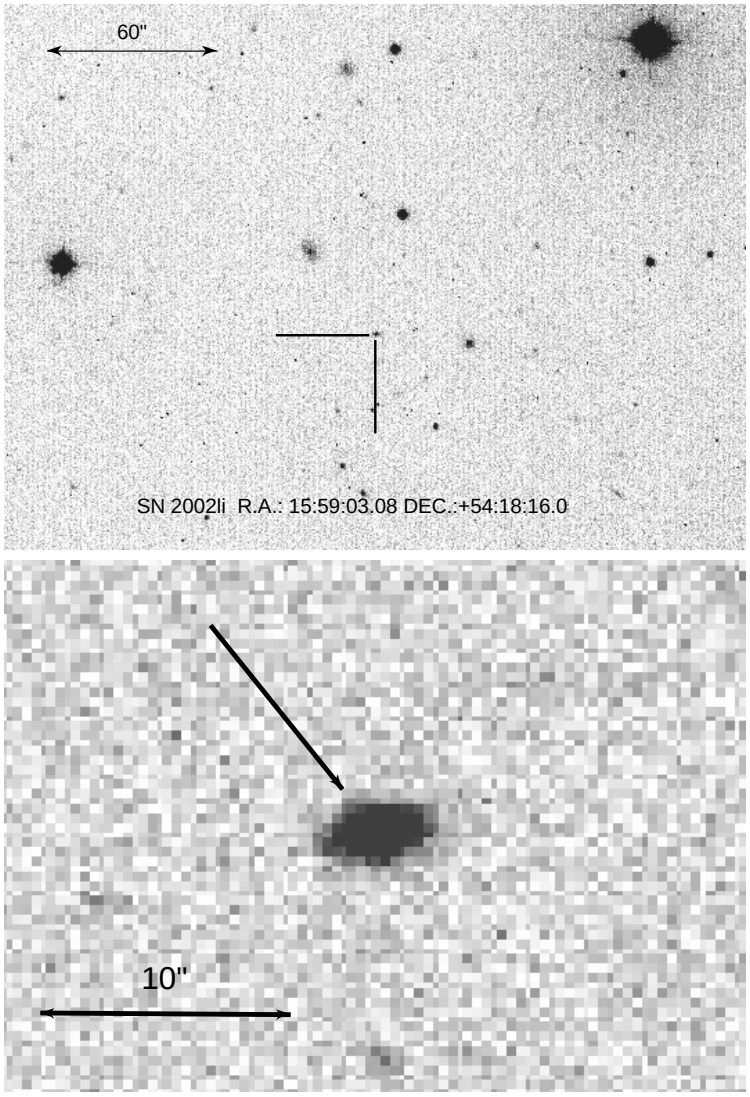

Fig. 1.— Top: Finding chart of SN 2002li. g' band image (exp. time : 600 sec) obtained on June 11, 2002 with the JKT 1.0-m telescope + JAG-CCD). Bottom: SN 2002li. INT+WFC, Jun 7, 2002, exp. time: 240 sec, g' band.

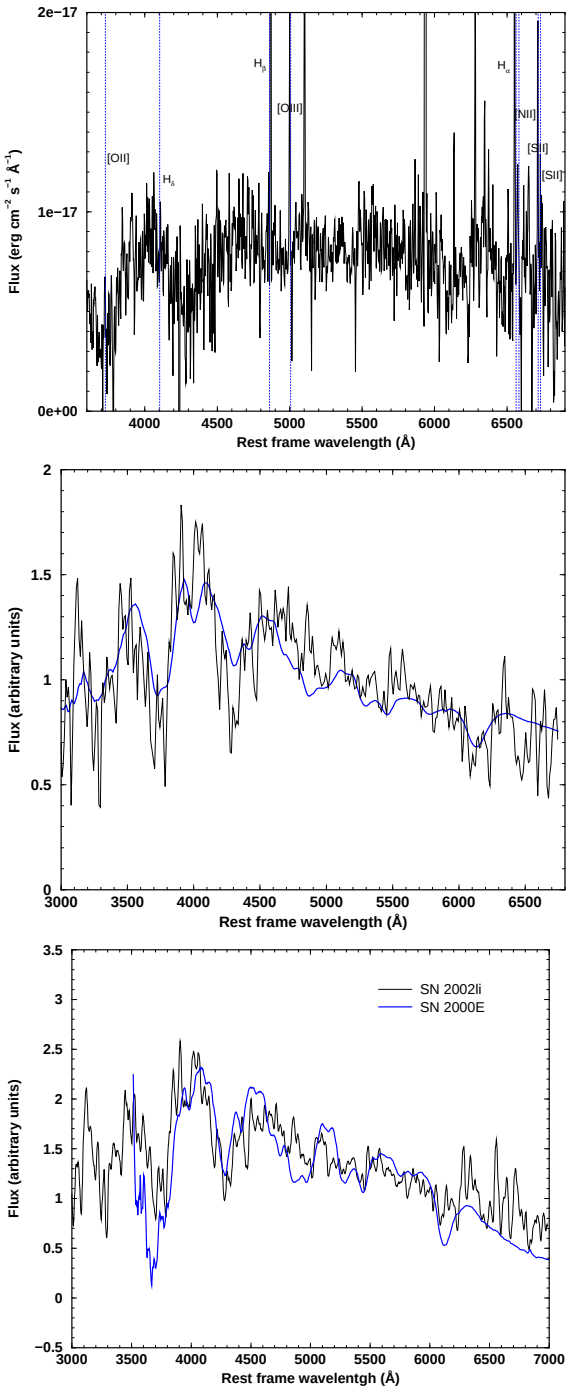

Fig. 2.— Top: Spectrum of SN 2002li, including galaxy lines for the redshift determination. Middle: Template fitting of SN 2002li spectrum. Template epoch is 2 days before maximum. SN 2002li spectrum has been dereddened and smoothed. Bottom: Comparison of SN 2002li smoothed spectrum with that of SN 2000E 4 days before maximum. Both SN 2002li and SN 2000E spectra have been dereddened and smoothed.

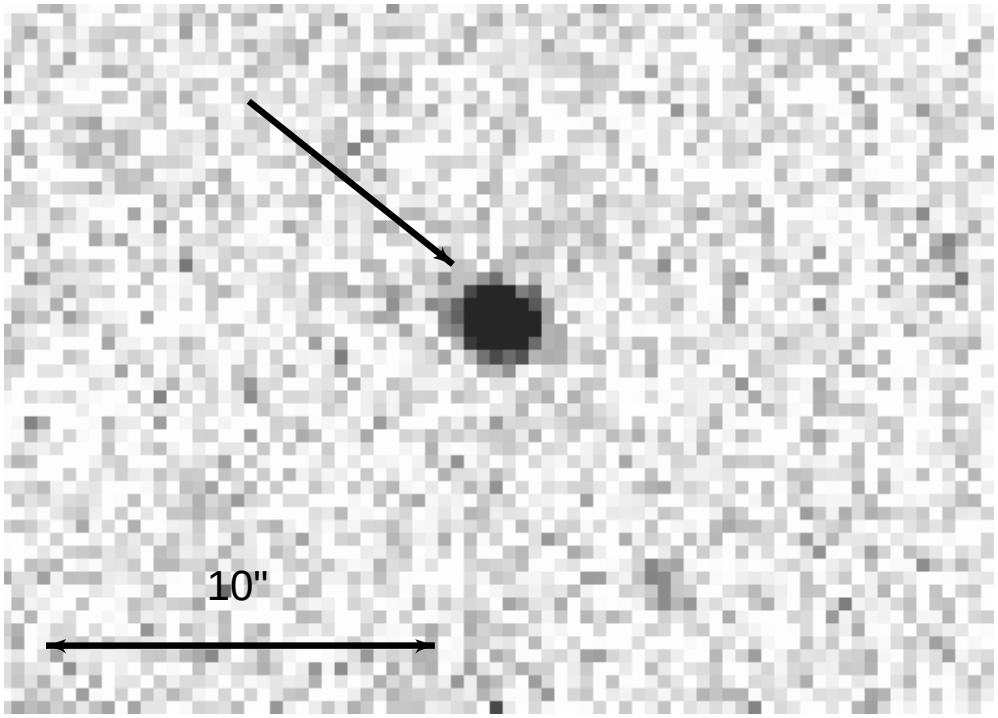

Fig. 3.— Top: Finding chart of SN 2002lj. g' band image (exp. time : 240 sec) obtained on June 5, 2002 with the INT telescope + WFC. Bottom: SN 2002lj, INT+WFC, Jun. 7, 2002, exp. time: 240 sec, g' band.

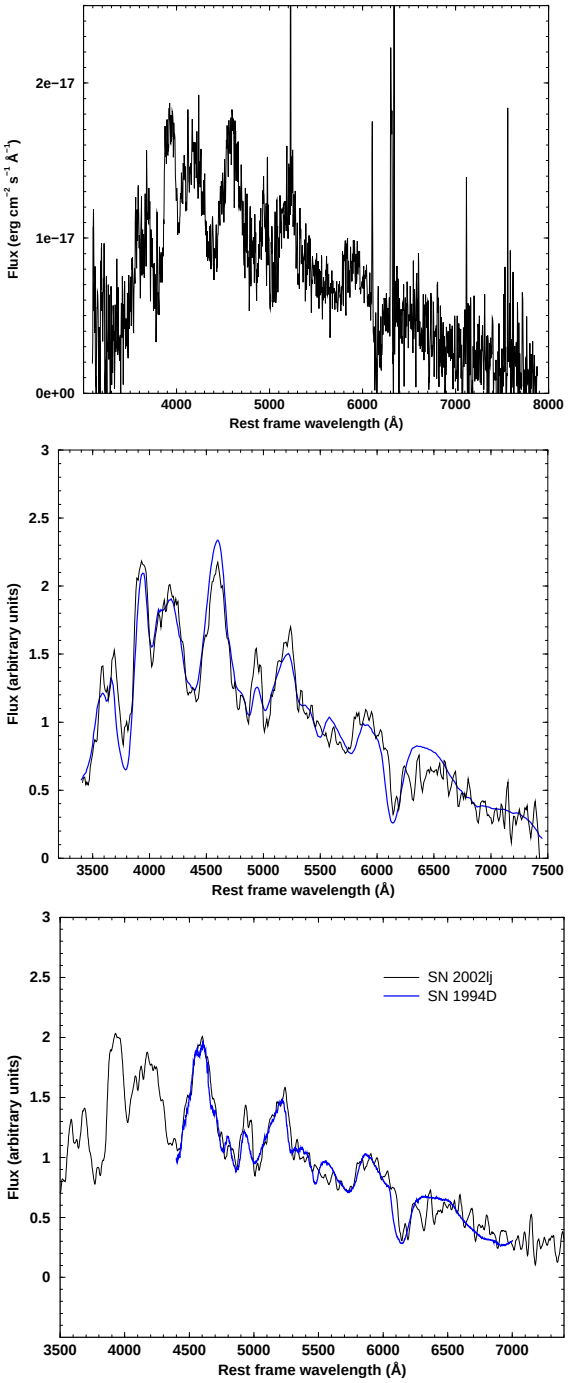

Fig. 4.— Top: Spectrum of SN 2002lj. No galaxy lines have been found. Redshift determined from supernovae features. Middle: Template fitting of SN 2002lj smoothed spectrum. Template epoch is 7 days past maximum. Bottom: Comparison of SN 2002lj spectrum with that of SN 1994D 7 days past maximum. Both spectra have been smoothed.

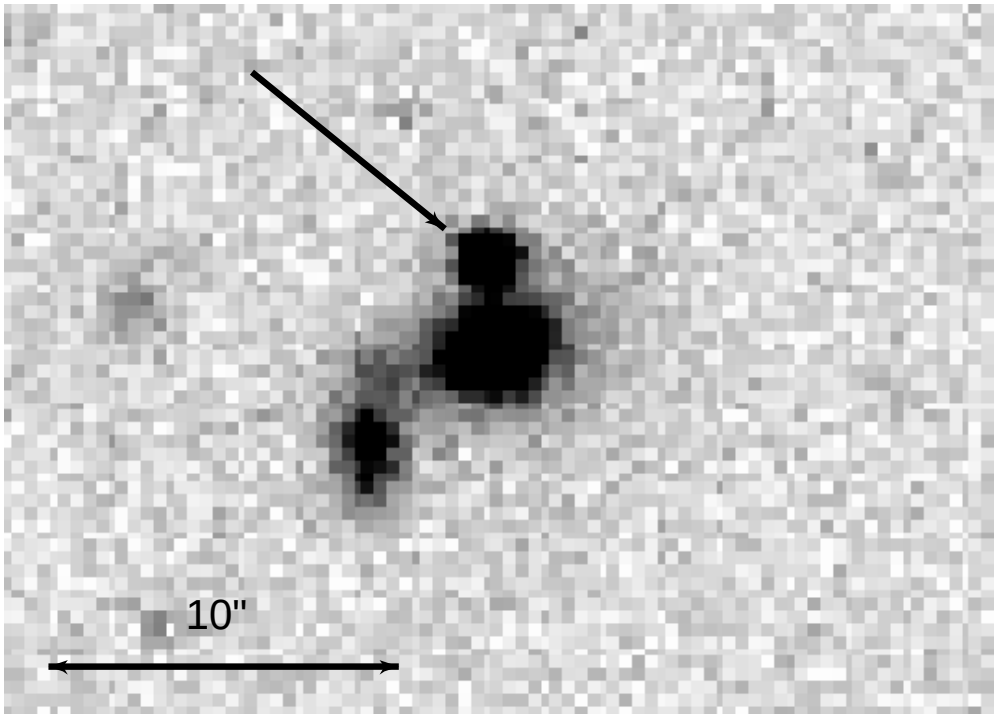

Fig. 5.— Top: Finding chart of SN 2002lp. g' band image (exp. time : 240 sec) obtained on June 5, 2002 with the INT telescope + WFC). Bottom: SN 2002lp, INT+WFC, Jun. 6, 2002, exp. time: 240 sec, g' band .

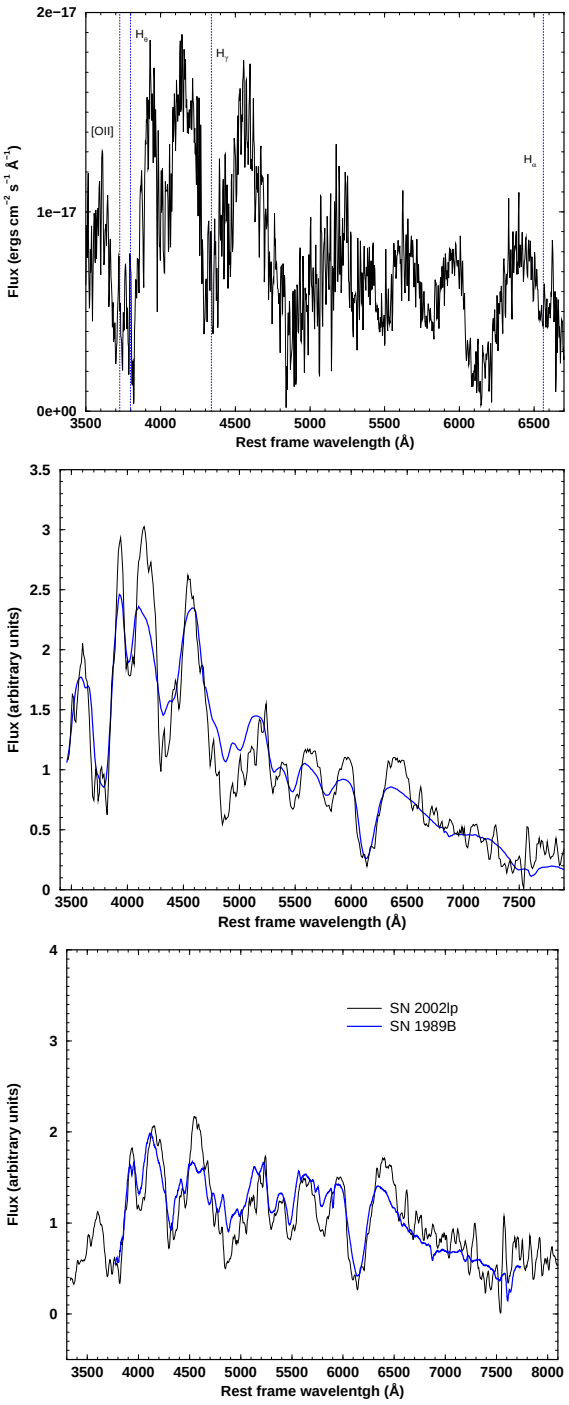

Fig. 6.— Top: Spectrum of SN 2002lp, including galaxy lines for the redshift determination. Middle: Template fitting of SN 2002lp spectrum. Template epoch is 3 days past maximum. SN 2002lp spectrum has been smoothed and dereddened. Bottom: Comparison of SN 2002lp spectrum with that of SN 1989B at maximum. SN 2002lp spectrum has been dereddened. Both spectra have been smoothed.

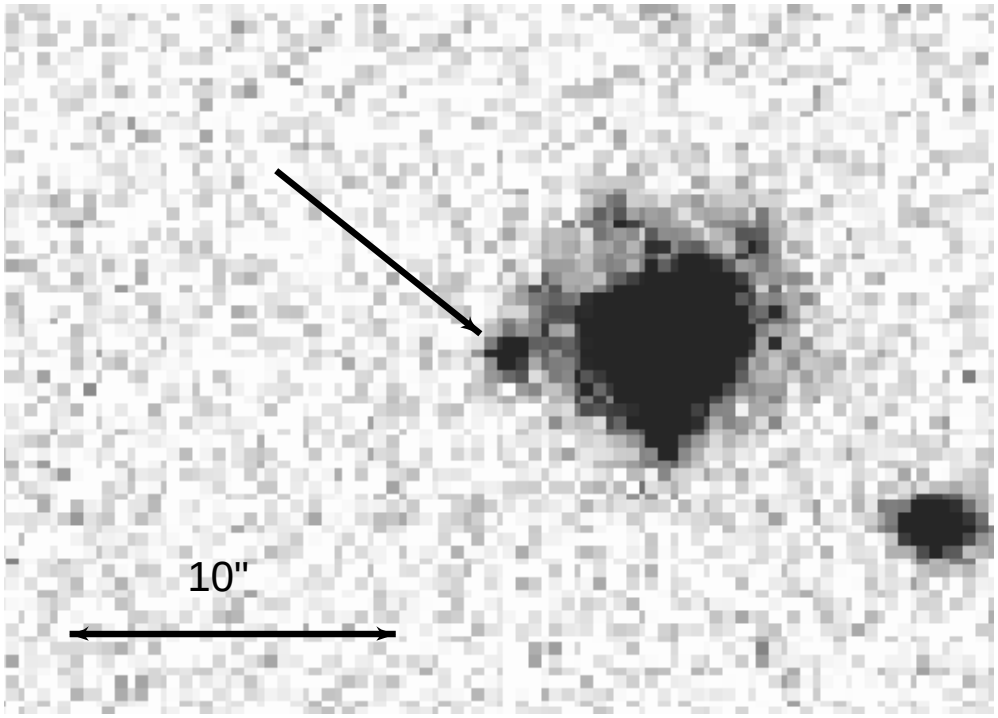

Fig. 7.— Top: Finding chart of SN 2002lq. g' band image (exp. time : 240 sec) obtained on June 8, 2002 with the INT telescope + WFC). Bottom: Same image zoomed to point at the supernova.

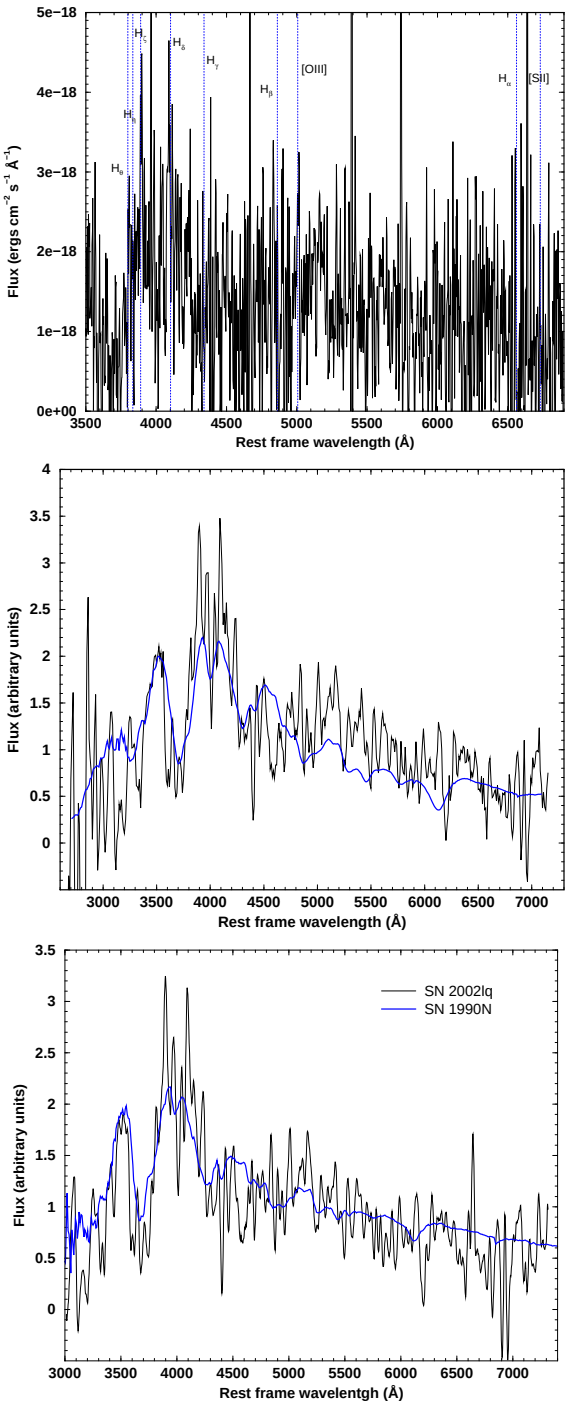

Fig. 8.— Top: Spectrum of SN 2002lq, including galaxy lines for the redshift determination. Middle: Template fitting of SN 2002lq spectrum. Template epoch is 7 days before maximum. SN 2002lq spectrum has been smoothed and dereddened. Bottom: Comparison of SN 2002lq spectrum with that of SN 1990N 7 days before maximum. SN 2002lq spectrum has been smoothed and dereddened.

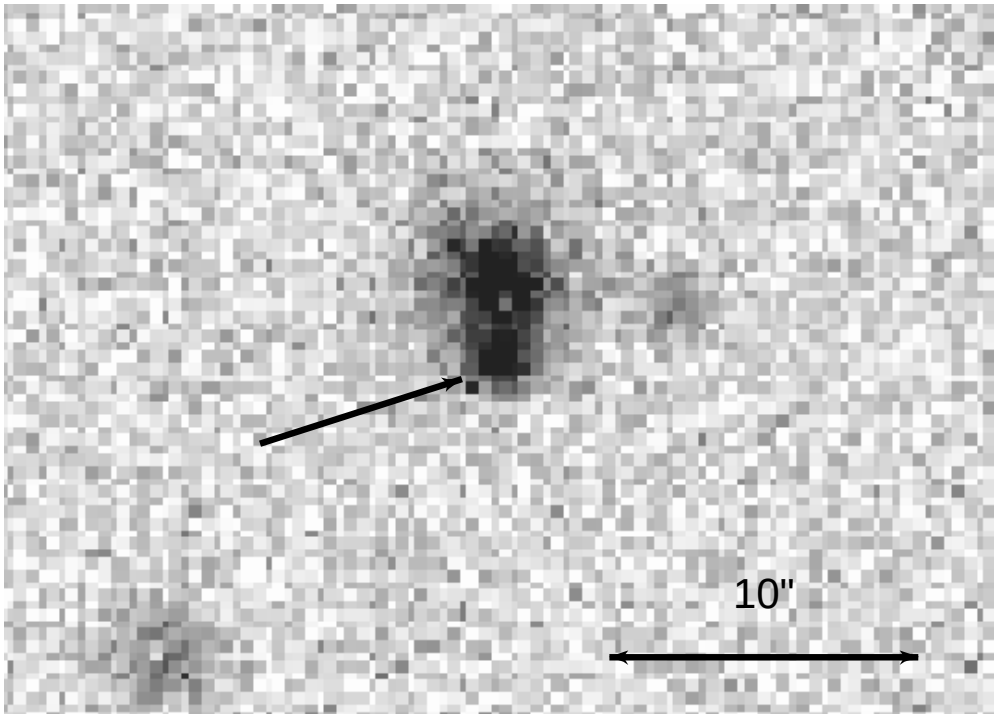

Fig. 9.— Top: Finding chart of SN 2002lr. g' band image (exp. time : 240 sec) obtained on June 6, 2002 with the INT telescope + WFC). Bottom: Same image zoomed to point out at the supernova.

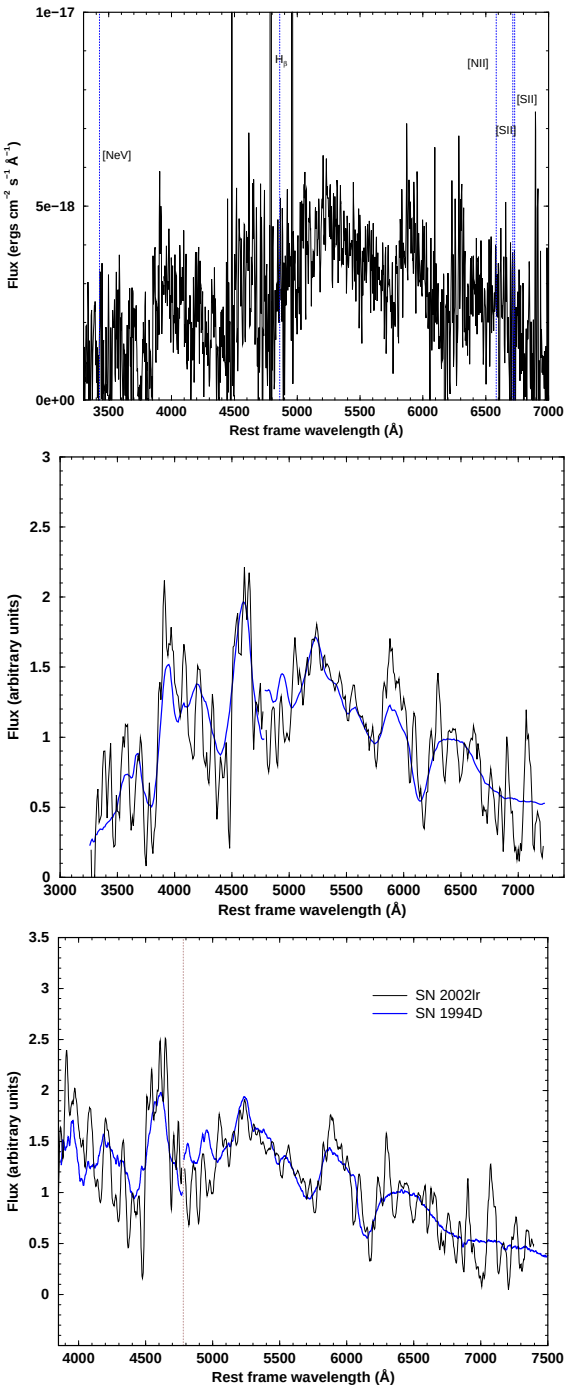

Fig. 10.— Top: Spectrum of SN 2002lr, including galaxy lines for the redshift determination. Middle: Template fitting of SN 2002lr smoothed spectrum. Template epoch is 10 days past maximum. Bottom: Comparison of SN 2002lr spectrum with that of SN 1994D 10 days past maximum. Both spectra have been smoothed.

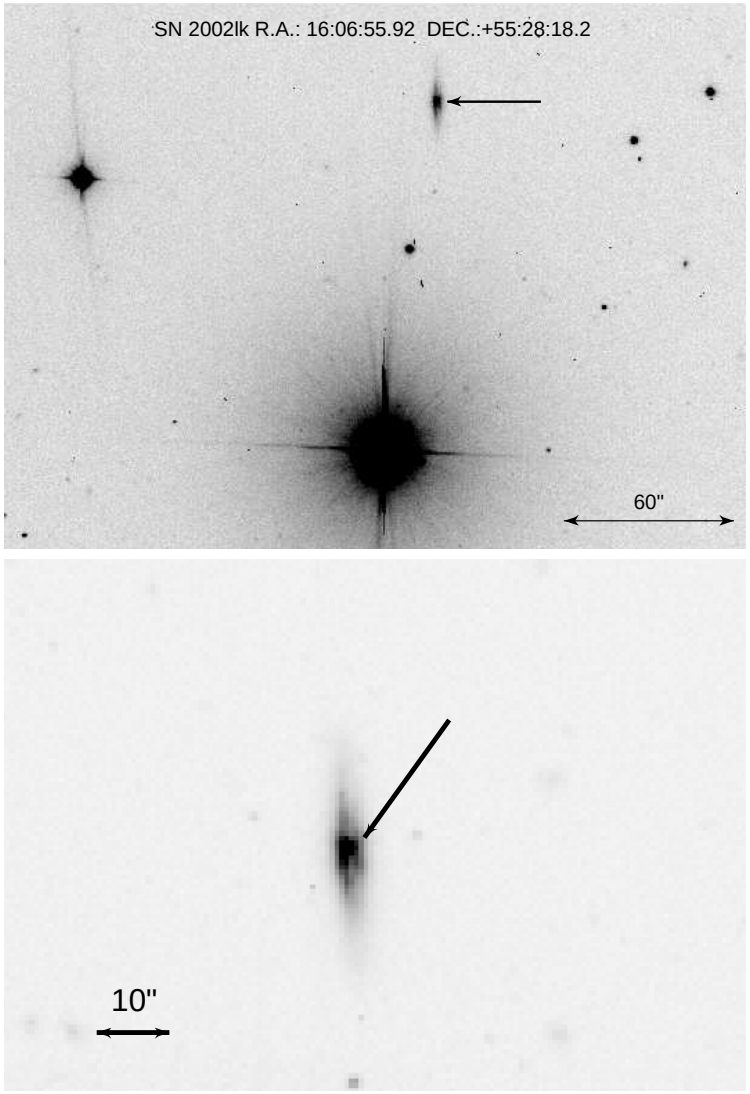

Fig. 11.— Top: Finding chart of SN 2002lk. g' band image (exp. time : 240 sec) obtained on June 7, 2002 with the INT telescope + WFC). Bottom: Same image zoomed to point out the supernova.

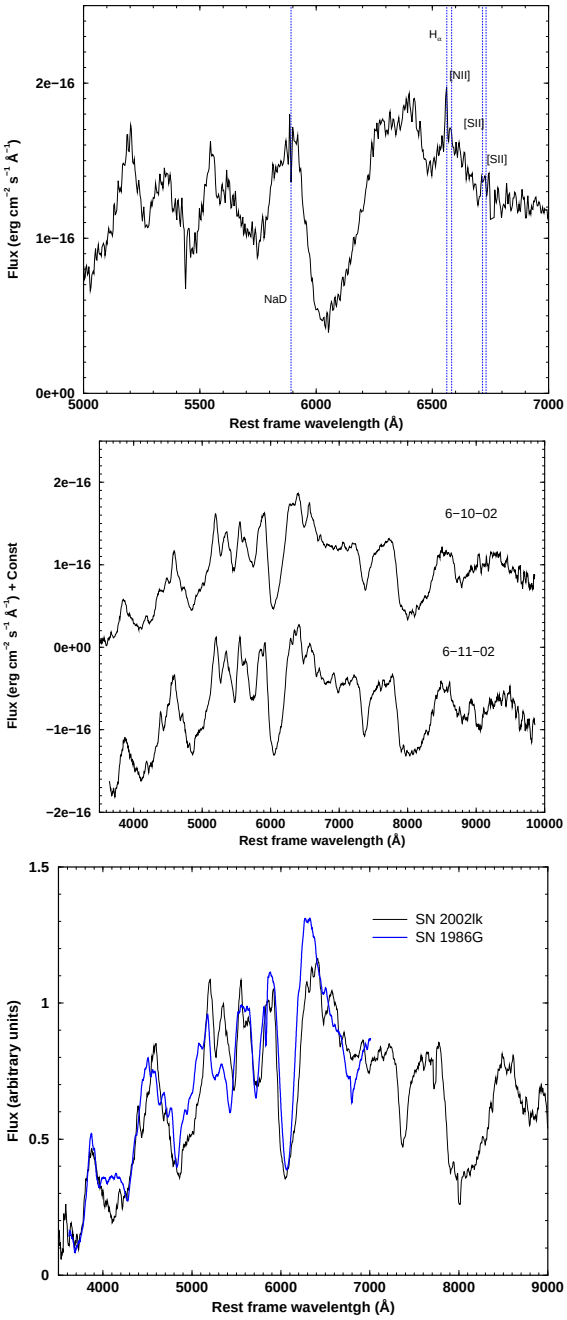

Fig. 12.— Top: Spectrum of SN 2002lk on June 10, including galaxy lines for the redshift determination. Spectra of SN 2002lk on June 10 and June 11 ($-2 \times 10^{-16} ergcm^{-2}s^{-1}$ Å^{-1}). Middle: Comparison of SN 2002lk spectrum on June 11 with that of SN 1991bg at maximum. Bottom: Comparison of SN 2002lk spectrum on June 11 with that of SN 1986G 2 days before maximum. SN 1986G spectrum has been smoothed.

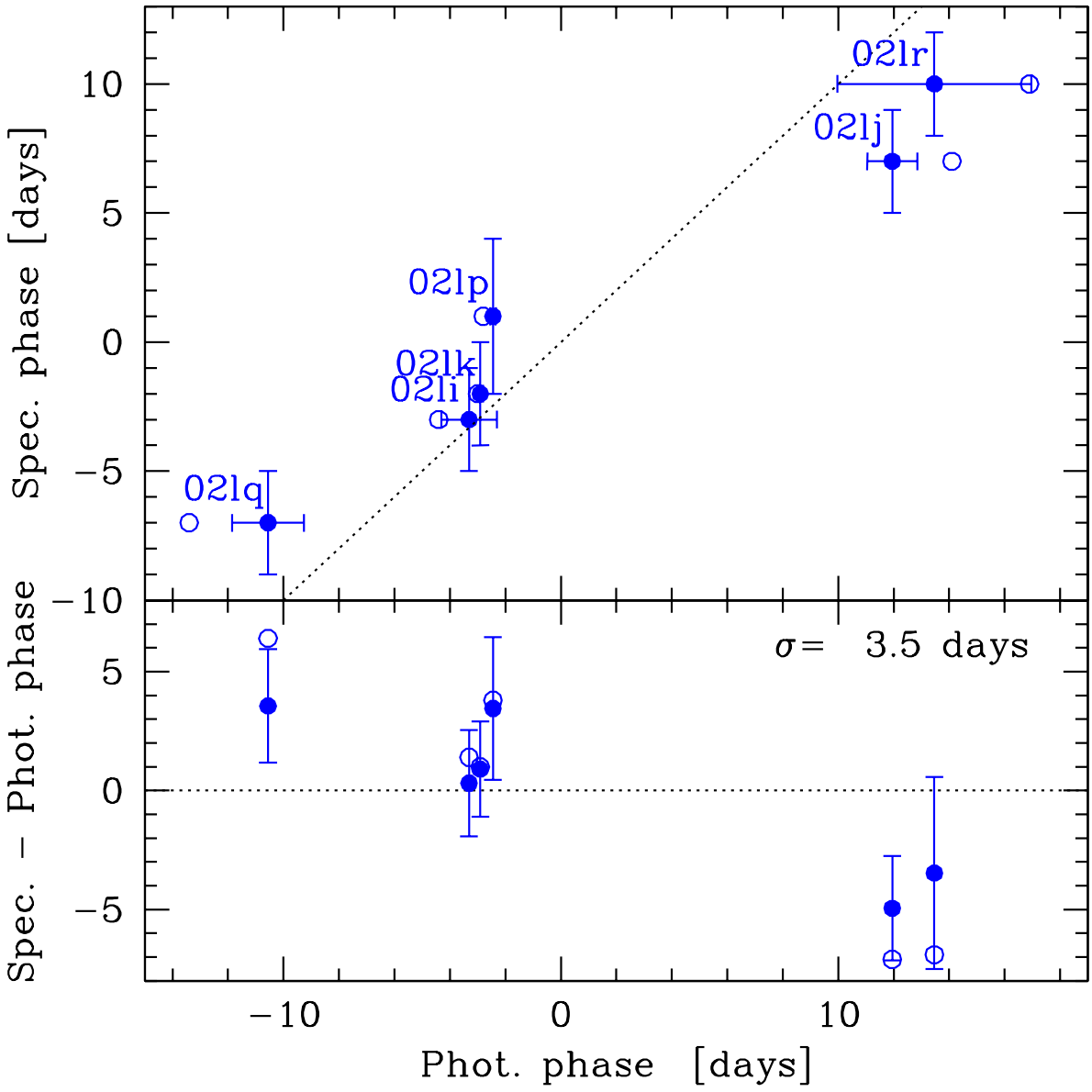

Fig. 13.— Comparison of the spectrum epochs as determined from the spectrum fits (τ_{spec}) and the light curve fits (τ_{pho}). Filled dots: τ_{pho} corrected for time dilation; empty dots: τ_{pho} not corrected for time dilation. Epochs are relative to the B band maximum. The dispersion σ is relative to the corrected points. The dotted line corresponds to $\tau_{spec} = \tau_{pho}$.

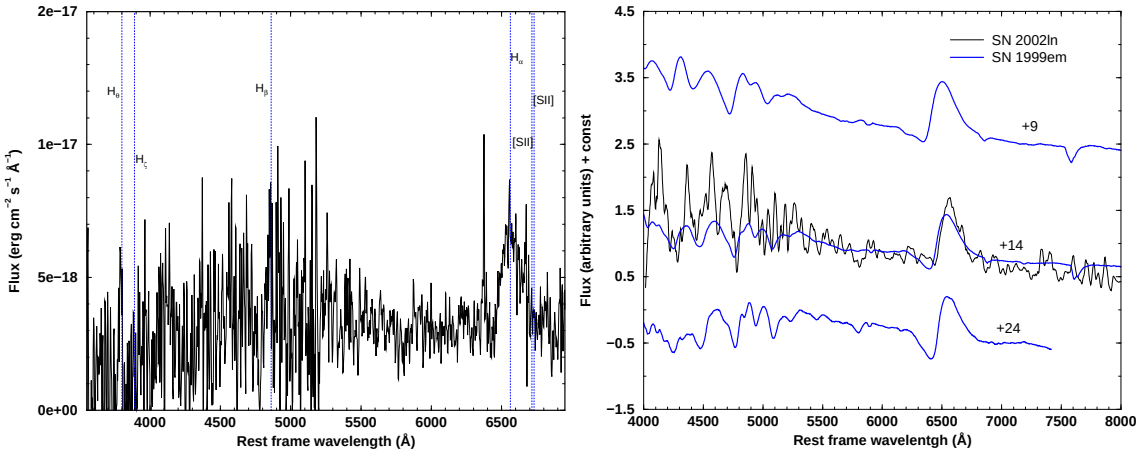

Fig. 14.— Left panel: Spectrum of the Type II supernova SN 2002ln, including galaxy lines for the redshift determination. Right panel: Comparison of SN 2002ln spectrum with that of SN 1999em about 9, 14, and 24 since B maximum. Both SN 2002ln and SN 1999em spectra have been smoothed.

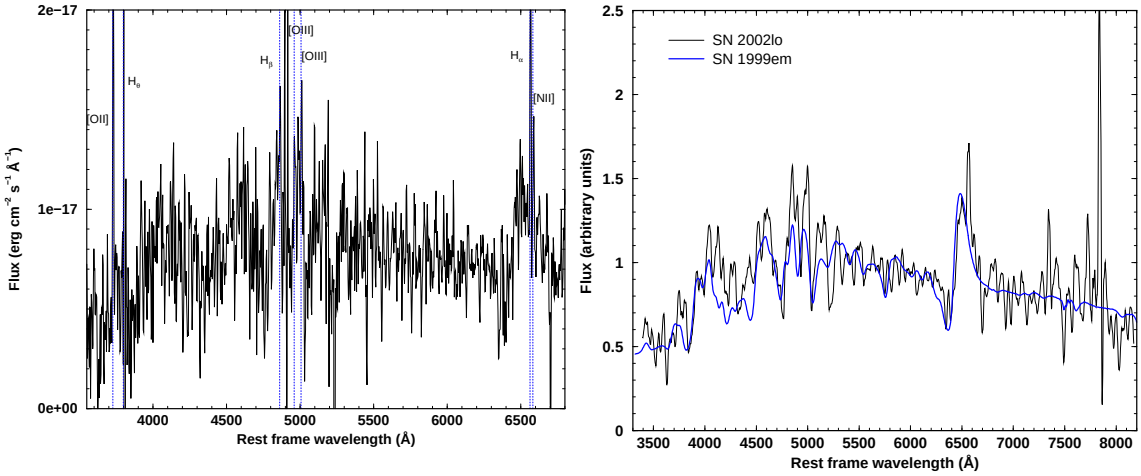

Fig. 15.— Left panel: Spectrum of the Type II supernova SN 2002lo, including galaxy lines for the redshift determination. Right panel: comparison of SN 2002lo spectrum with that of SN 1999em ∼35 days since B maximum. Both SN 2002lo and SN 1999em spectra have been smoothed.

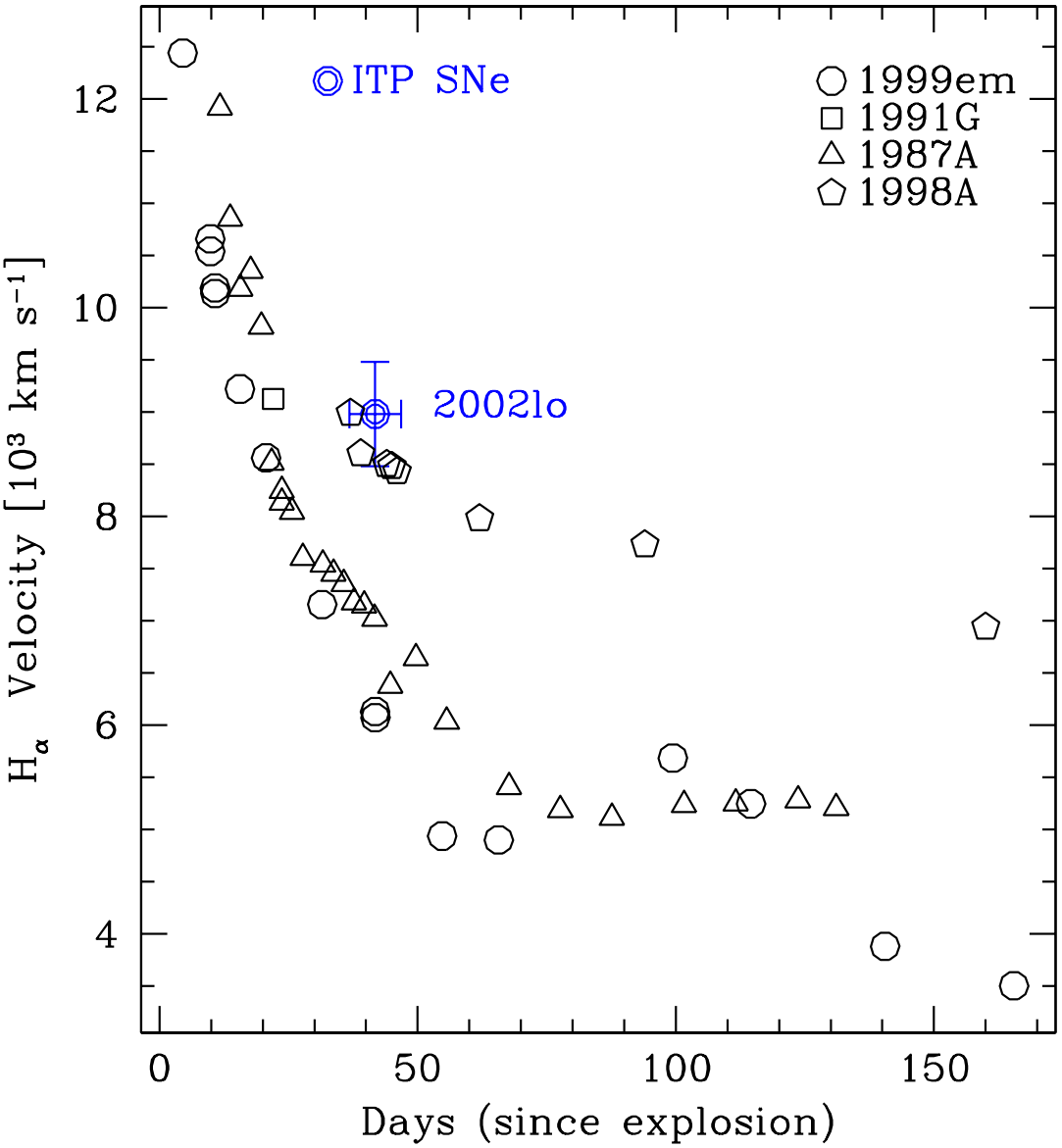

Fig. 16.— Expansion velocity for H_α (6562.8 Å) as deduced from its minimum, in SN 2002lo, compared with those of SN 1999em (Elmhamdi et al. 2003), 1991G (Blanton et al. 1995), 1987A (Phillips et al. 1989), and 1998A (Pastorello et al. 2005).

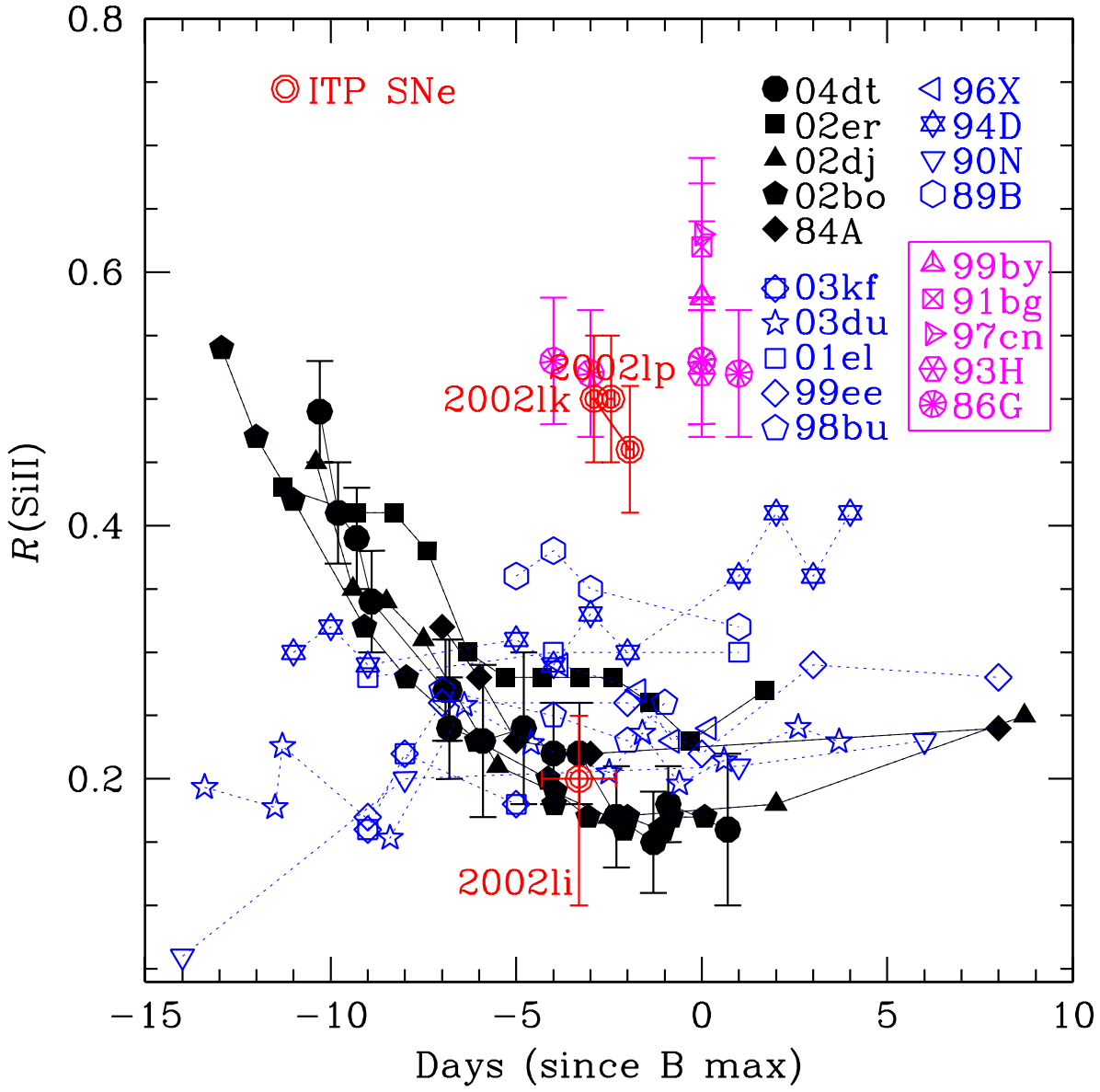

Fig. 17.— $\mathcal{R}$(Si II) parameter for SN 2002lk, SN 2002lp and SN 2002li, and for a sample of nearby SNe shown as comparison. Filled symbols refer to High Velocity Gradient SNe, open symbols to Low Velocity Gradient SNe as defined in Benetti et al. (2005). FAINT SNe, listed in the box, are also shown.

XC

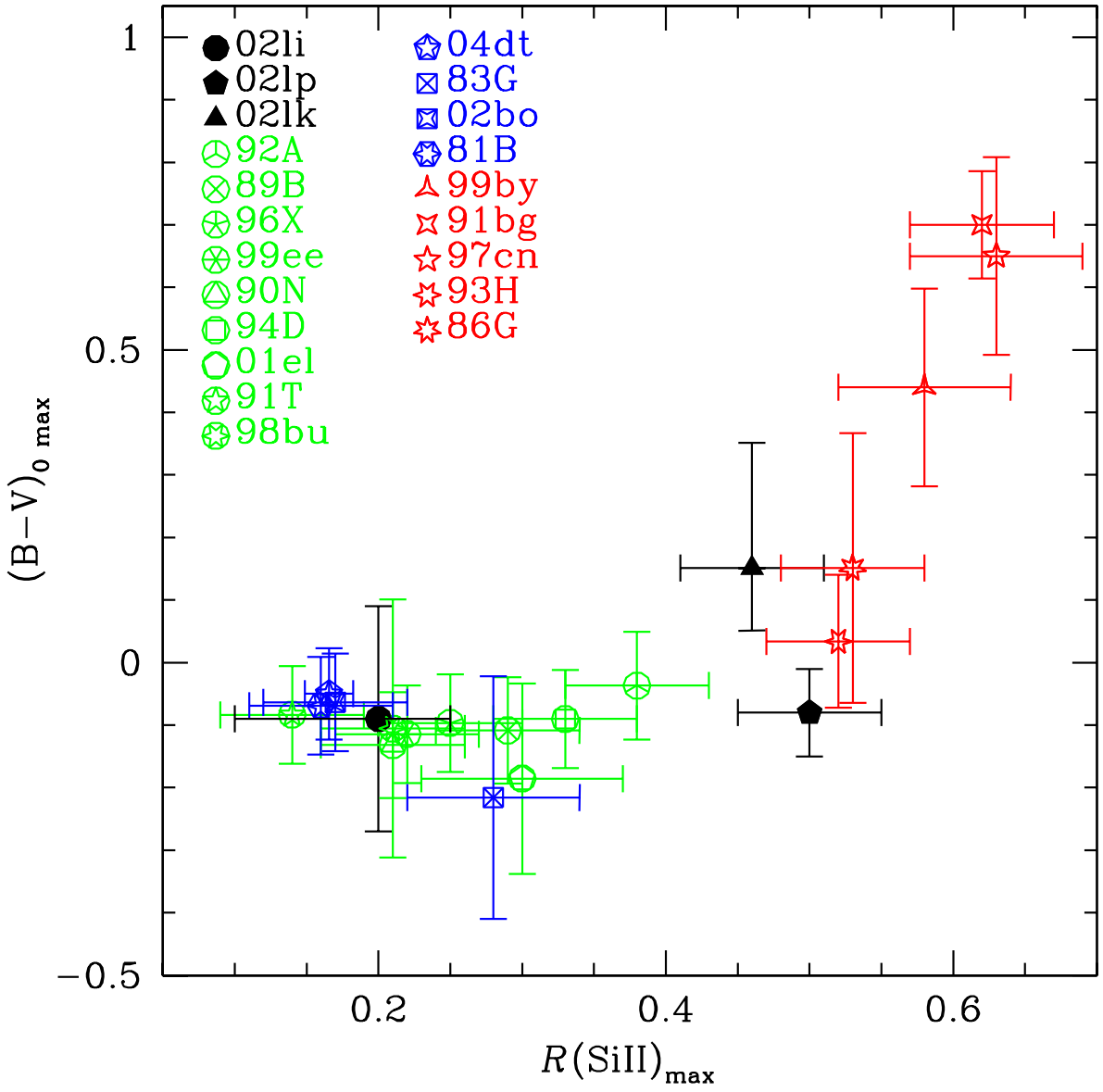

Fig. 18.— $\mathcal{R}$(Si II) parameter and intrinsic (B-V).

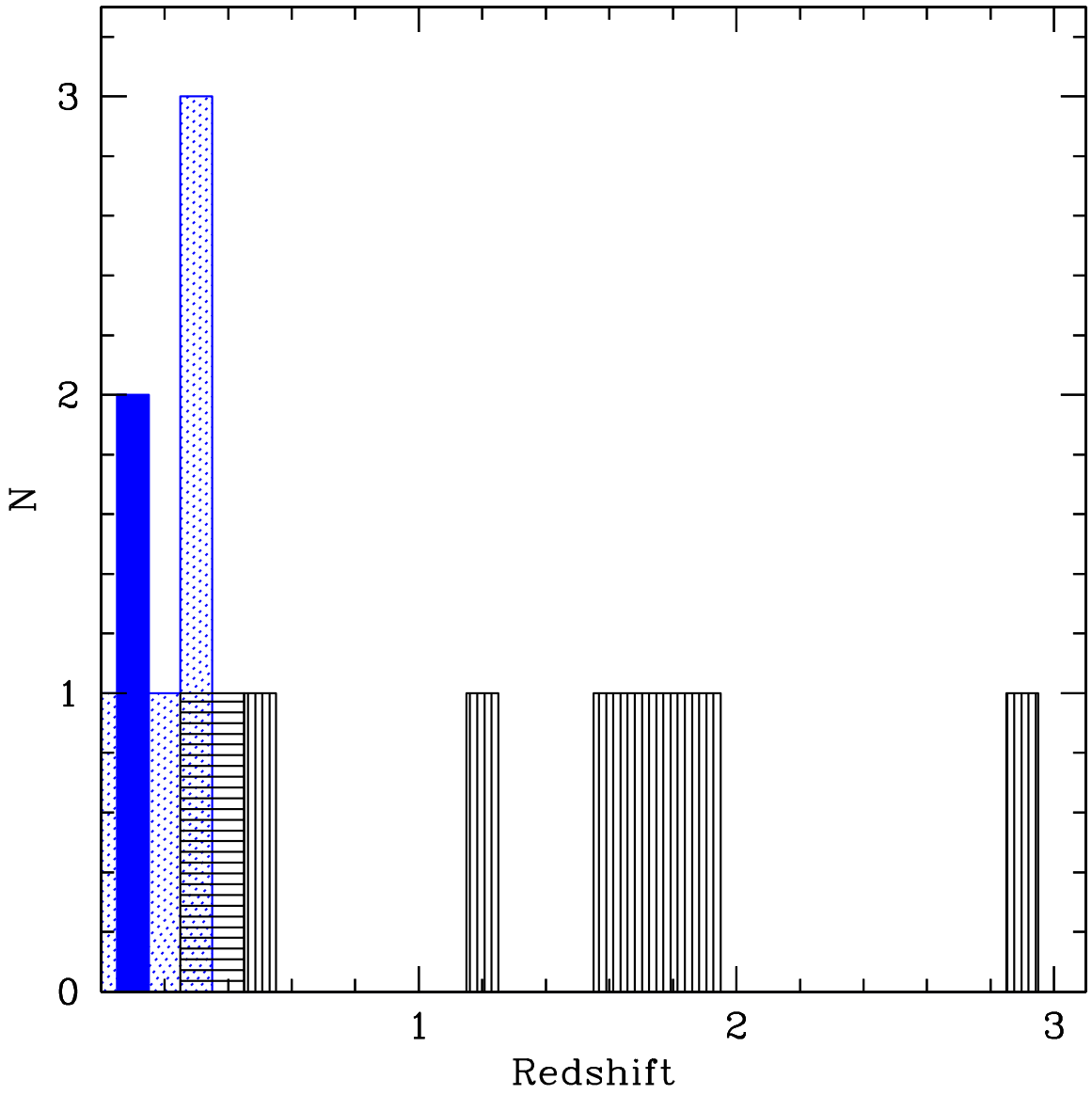

Fig. 19.— Redshift distribution of the observed objects. Filled histogram: Type II SNe; dotted histogram: Type Ia SNe; horizontal line histogram: Seyfert galaxies; vertical lines histogram: QSOs. redshift bin: 0.1.

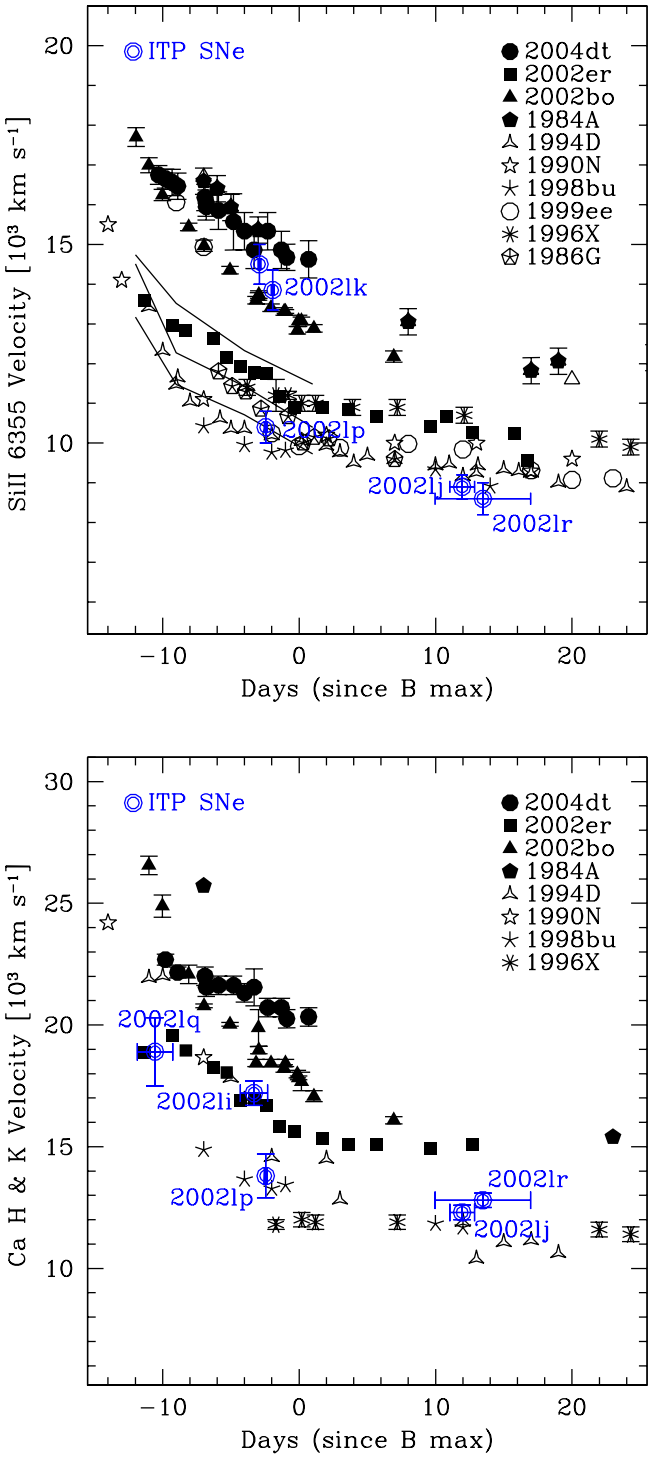

Fig. 20.— Expansion velocities for Si II (6355 Å) (upper panel) and Ca II (3950 Å) (lower panel) as deduced from their minima, compared with those of other SNe. The Si II evolution expected for different metallicities (solid line, top: ×10 solar metallicity; middle: ×1; bottom: ×0.1) is also shown (Lentz et al. 2000). The phase has been determined from the light curve fitting.

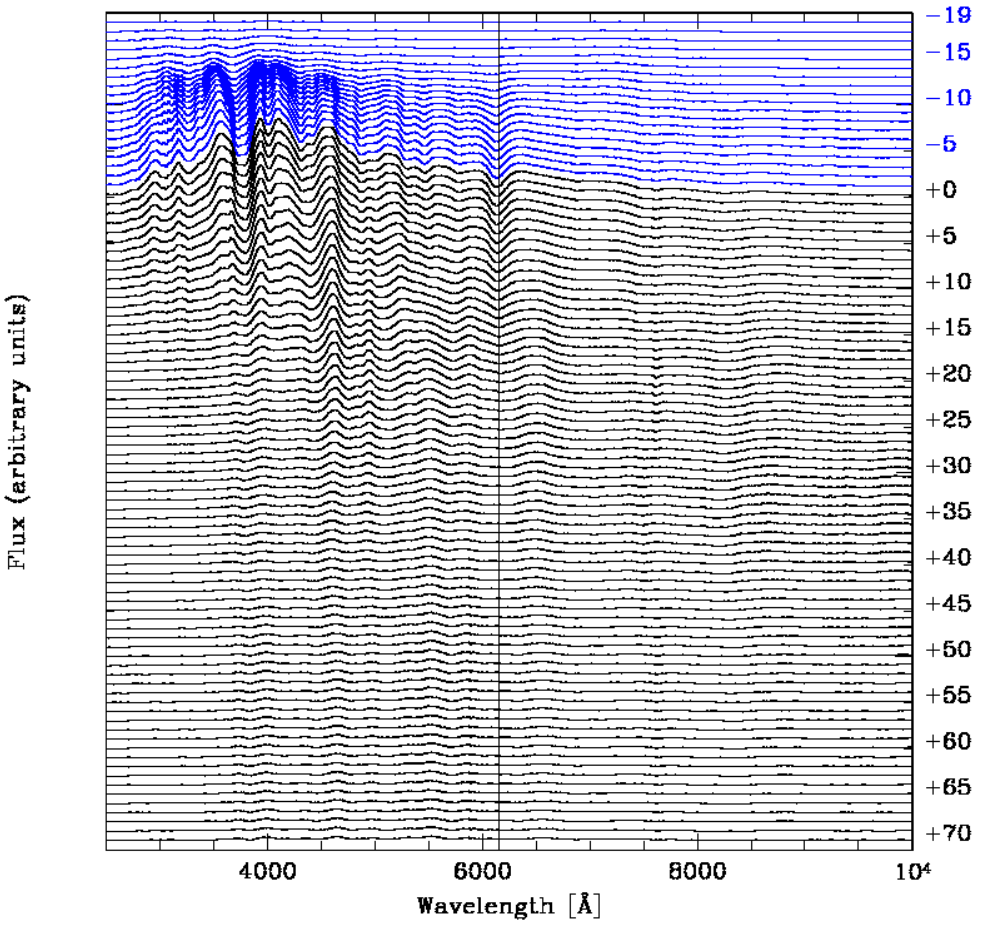

Fig. 21.— Synthetic spectra by Nobili et al. (2003). A vertical line marks the position of the Si II λ6150 absorption. Wavelength range limited to 2500–10000 Å. Phases are shown on the right.

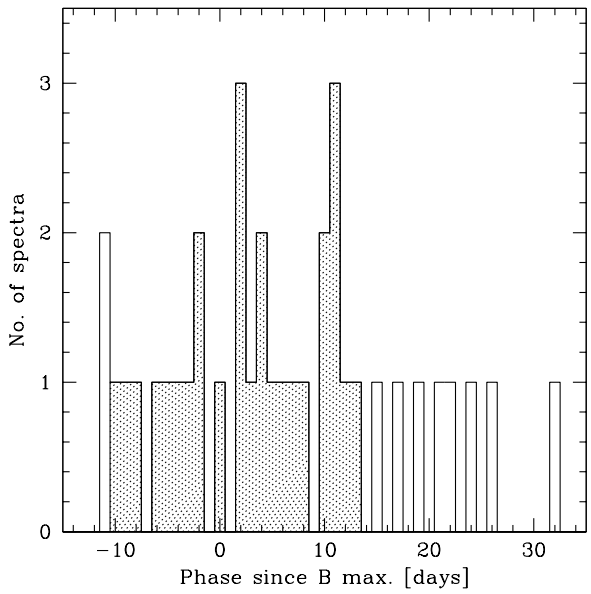

Fig. 22.— Phase distibution of the normal SN Ia templates listed in Table 5 (limited to 35 days since B maximum). The dotted area shows the phase range of our SN Ia sample. Phase bin: 1 day.